doi:10.1111/j.1440-1746.2007.05041.x

HEPATOLOGY

Transforming growth factor-α accelerates hepatocyte repopulation after hepatocyte transplantation

Takashi Kosone,* Hitoshi Takagi,* Norio Horiguchi,* Satoru Kakizaki,* Ken Sato,* Yoshifumi Watanabe† and Masatomo Mori*

*Department of Medicine and Molecular Science, Gunma University Graduate School of Medicine, Maebashi; and †Department of Biomolecular Engineering, Tokyo Institute of Technology, Yokohama, Japan

Key words
apoptosis, hepatocyte transplantation, transforming growth factor-α.

Accepted for publication 4 March 2007.

Correspondence
Associate Professor Hitoshi Takagi, Department of Medicine and Molecular Science, Gunma University Graduate School of Medicine, 3-39-15 Showa-machi, Maebashi, Gunma 371-8511, Japan. Email: htakagi@med.gunma-u.ac.jp

Abstract

Background and Aim: Although hepatocyte transplantation could be an alternative to orthotopic liver transplantation, many problems, such as rejection, location, required volume, and hepatocyte activity are currently unresolved. We previously demonstrated an anti-apoptotic effect in transgenic mice overexpressing transforming growth factor (TGF)-α. We herein present the details of a successful hepatocyte transplantation using TGF-α transgenic mice.

Methods: We used transgenic (TG) mice which overexpressed human TGF-α controlled by the metallothionein promoter. Wild-type mice were used as the controls (WT). Parenchymal hepatocytes were isolated from an adult mouse by the modified *in situ* perfusion method. The proliferation and resistance to Fas-induced apoptosis were examined *in vitro*. In addition, we transplanted the parenchymal hepatocytes into the peritoneal cavity of the WT mice.

Results: The TG hepatocytes showed higher proliferative activity and more resistance to Fas-induced apoptosis in comparison to the WT hepatocytes. Moreover, an immunohistochemical analysis demonstrated that the transplanted TG hepatocytes increased more in size and showed a higher expression of CD31 and vascular endothelial growth factor in comparison to the WT hepatocytes. We also observed that albumin was expressed in equal amounts in both types of transplanted hepatocytes.

Conclusion: Cell transplantation with TGF-α overexpressing hepatocytes could preserve hepatocyte function.

Introduction

Hepatocyte transplantation has been the subject of laboratory investigations for over 20 years and is now partially available for the treatment of liver disease. A number of experiments have demonstrated the feasibility of total liver parenchymal cell replacement by transplanted hepatocytes.[1–4] However, researchers are still looking for more efficient methods of hepatocyte transplantation to employ for clinical treatments. Normal hepatocytes can be an ideal cell source for hepatocyte transplantation, but very few healthy donor cells are available. Researchers have therefore tried to increase cell numbers by culturing hepatocytes. Because matured hepatocytes do not proliferate well under classical culture conditions, various strategies have been employed to increase the cell numbers. These strategies include attempting to develop immortal cells by gene transduction and searching for hepatic stem cells or an alternative stem cell source that will transdifferentiate into hepatocytes.[5–7]

The hepatocytes of various mouse models have also been utilized to enhance the rate and degree of hepatocyte repopulation.[8–12]

We previously demonstrated the presence of anti-apoptotic activity in transgenic (TG) mice overexpressing transforming growth factor (TGF)-α.[13,14] In this study, the hepatocytes of TGF-α transgenic mice showed a high proliferative ability and a resistance to apoptosis. Moreover, we demonstrated the acceleration of the hepatocyte repopulation after intraperitoneal transplantation of the hepatocytes of TGF-α transgenic mice. Our data demonstrated that these hepatocytes could effectively induce hepatocyte repopulation and suggested that TGF-α accelerates liver reconstitution *in vivo*.

Methods

Transgenic mice

The transgenic mouse line MT100 bearing the metallothionein-TGF-α fusion gene was created as described previously.[15,16] In this study, we used 6- to 8-week-old, male MT100 mice (TG) and non-transgenic littermates (wild type [WT]). All the animal studies

Journal of Gastroenterology and Hepatology 23 (2008) 260–266

were performed according to the guidelines for animal care and use established by Gunma University Graduate School of Medicine (Maebashi, Japan).

Cell preparation

Parenchymal hepatocytes were isolated from an adult mouse by the modified *in situ* perfusion method.[17] Briefly, the liver was perfused *in situ* through the thoracic inferior vena cava with 0.0125% collagenase solution. The liver was subsequently dissected and removed and the cells were dispersed in cold Hanks' solution. Parenchymal hepatocytes were separated from nonparenchymal cells by differential centrifugation at 50 *g* for 90 s. Dead parenchymal hepatocytes were removed by density gradient centrifugation on Percoll (GE Healthcare UK, Giles, UK). Morphologically, more than 95% of the cells were hepatocytes. The initial rate of viability was approximately 90%, as assessed by cell membrane exclusion of trypan blue dye. Plating efficiency was determined to further evaluate cell quality. The parenchymal hepatocytes were suspended in Williams' E medium and were plated in bovine serum albumin-coated plates. The purity of the hepatocytes was confirmed by microscopic observation.

Analysis of cell growth

Primary hepatocytes were incubated at 37°C in a humidified chamber of 5% CO_2. The hepatocytes were seeded in 96-well microtiter plates (Nunc, Napervill, IL, USA) at a cell density of 2×10^4 cells/0.1 mL/well. The hepatocytes were cultured in Williams' E medium (Sigma, St Louis, MO, USA), and epidermal growth factor (EGF, 50 ng/mL, Upstate Biotechnology, Lake Placid, NY, USA) was added to the one dish of WT hepatocytes. The final EGF concentration for this treatment was determined by previous studies.[18,19] The microtiter plates were incubated for 24, 48, 72, and 120 h. The cell growth was measured by a 3-(4, 5-dimethylthiazol-2-yl)-2,5-diphenyl tetrazolium bromide assay (Sigma, USA). The number of viable cells was estimated by measuring the absorbance (optical density 550 values) in a microplate reader at 550 nm with a reference wavelength of 650 nm. Hepatocyte proliferation examination was performed six times by repeating experiments.

RNA analysis

The total cellular RNA was extracted using Isogen (Nippon Gene, Toyama, Japan) according to the protocol recommended by the manufacturer. A sample of 20 μg total RNA was fractionated by electrophoresis through 1% agarose gel and then blotted onto Hybond-N nylon membranes (GE Healthcare UK, UK), followed by UV cross linking. Hybridization was carried out at 42°C for 12 h. The TGF DNA probe was the human TGF-α cDNA (917 bp) labeled with (α-^{32}P) deoxycytidine triphosphate. This probe recognizes human TGF-α mRNA, but not mouse TGF mRNA. On the other hand, the DNA probe of vascular EGF (VEGF), an endothelial cell-specific growth factor involved in angiogenesis,[20–22] recognizes mouse VEGF mRNA and mouse Fas.[23,24] Northern blotting of hepatocytes was performed four times by repeating experiments.

In situ analysis of hepatocyte apoptosis by terminal deoxynucleotidyl transferase-mediated deoxyuridine triphosphate biotin nick end labeling assay

The terminal deoxynucleotidyl transferase-mediated deoxyuridine triphosphate biotin nick end labeling (TUNEL) assay was performed to detect apoptotic cells. After confirming cell viability by trypan blue dye, parenchymal hepatocytes isolated from mice by the *in situ* perfusion method were seeded on a Laboratory-Tek Chamber Slide (Nalge Nunc International, Rochester, NY, USA). These chamber slides were incubated for 48 h. Subsequently, mouse monoclonal agonistic Fas antibodies (0.5 μg/mL, Jo2, BD Pharmingen, Franklin Lakes, NJ, USA) were added. EGF (1 μg/mL) was added to the WT hepatocytes 1 h before adding the Fas antibodies. After the hepatocytes were washed with Williams' E medium, the 3'-hydroxyl ends of the DNA fragments were stained by the method described by the manufacturer (*In situ* apoptosis detection kit, ApopTag Direct, Oncor, Gaithersburg, Germany). The sections were viewed and photographed by standard fluorescence microscopy techniques. The TUNEL-positive cells were counted in five randomly-selected fields.

Spheroid formation and transplantation

The spheroid formation of hepatocytes was performed according to the method described previously.[25] Briefly, freshly isolated hepatocytes were cultured on a hydrophobic plate for 48 h, which resulted in the formation of spheroidal hepatocytes.[25] The hepatocytes were collected by gentle pipetting and cultured with Cytodex3 (Amersham Pharmacia Biotech AB, Uppsala, Sweden) beads (45 mg) on siliconized plates for 6 h using the method described previously.[26] The formed aggregates were harvested by gentle pipetting and suspended in 250 μL of Williams' E medium. The cell suspensions derived from WT and TG (WT hepatocytes and TG hepatocytes) were intraperitoneally injected into WT mice into the area adjacent to the pancreas. The formed aggregates were dissected 2 weeks after transplantation and examined. Hepatocyte transplantations were performed using five samples in the WT and TG groups.

Immunohistochemistry

The transplants were dissected and fixed overnight in 4% paraformaldehyde solution at 4°C. The tissues were embedded in Tissue-Tek compound (Miles Laboratories, Elkhart, IN, USA) and frozen in liquid nitrogen for preparation of the cryostat sections. The 10-μm sections were stained with antibodies after overnight blocking by fetal calf serum. The detection of the immunostained cells was performed by the avidin–biotin–peroxidase method using the ABC kit (Vector Laboratories, Burlingame, CA, USA), according to the instructions provided by the manufacturer. All the sections were lightly counterstained with 0.1% hematoxylin. Mouse immunoglobin G for a negative control was purchased from DAKO (Glostrup, Denmark). Goat antimouse albumin antibodies were purchased form Bethyl Laboratories (Montgomery, TX, USA). To evaluate microvessel density, we used anti-CD31 antibodies[27,28] (BD Pharmingen, USA) and an anti-VEGF

antibody[20–22] (Santa Cruz Biotechnology, Santa Cruz, CA, USA). Immunostaining was performed according to the usual methods and the immunostained-positive area was measured using the image software program (National Institute of Health, Bethesda, MD, USA) of the National Institute of Health in five microscopic fields at a 200-fold magnification and the mean ± SD were calculated. The scale was shown as the percentage of the positive area in the total area minus the Cytotex3 beads area. In the immunohistochemistry examination, one typical slide was shown out of three slides using anti-CD31 or anti-VEGF.

Statistical analysis

The data were expressed as mean ± SD. Differences between two groups were analyzed by Student's *t*-test. Differences between three groups were analyzed by one-way ANOVA statistics followed by the Student–Newman–Keuls test. The threshold for significance was set at $P < 0.05$.

Results

Expression of TGF-α transgene and VEGF in the primary hepatocytes

The TGF-α transgene was detected only in the TG hepatocytes (Fig. 1a). Moreover, VEGF was also detected in only the TG hepatocytes. These results demonstrated that the TG hepatocytes had higher potential for cell growth and vascular formation than the WT hepatocytes.

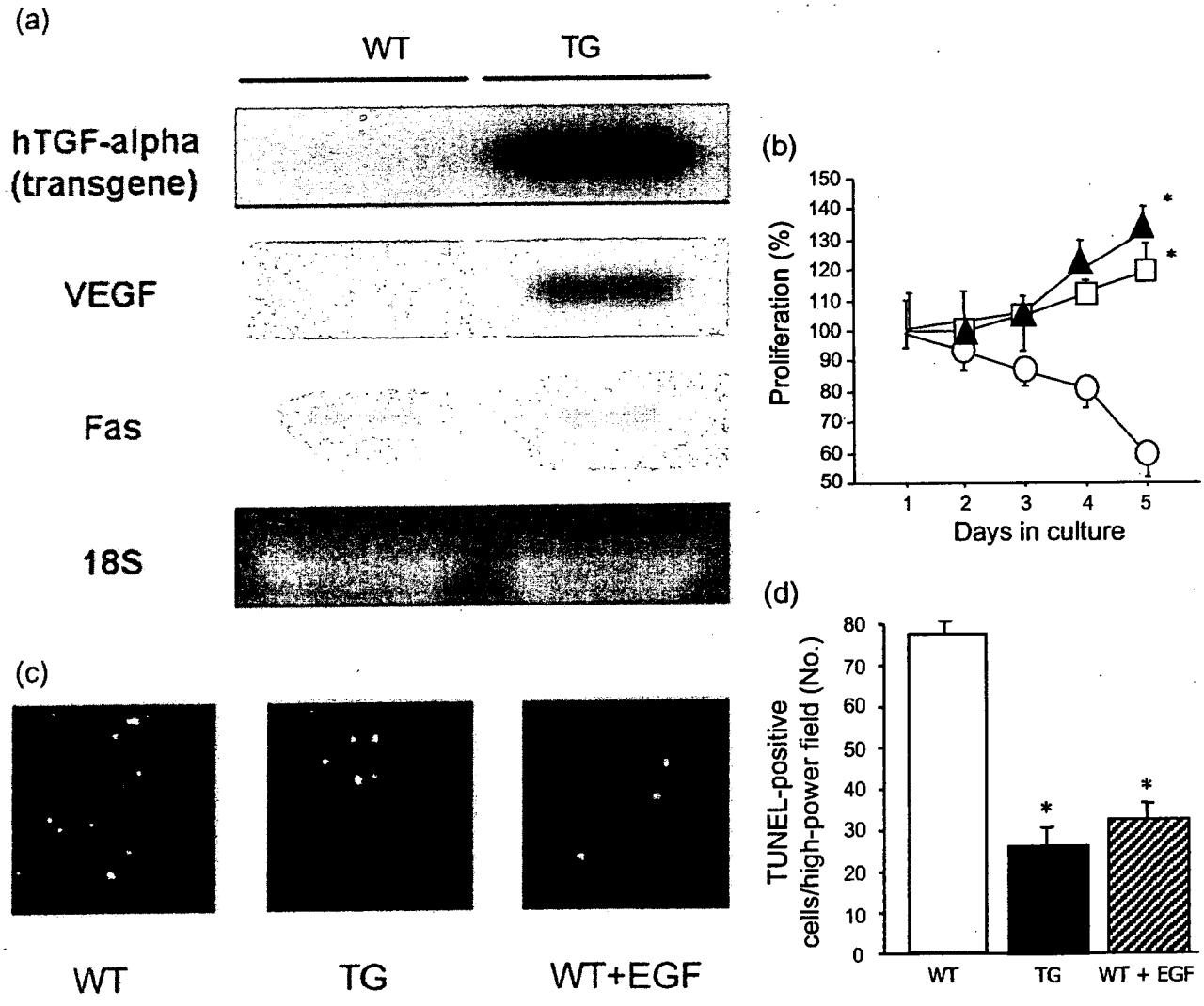

Figure 1 (a) Northern blot analysis of transforming growth factor-α (TGF-α), vascular epidermal growth factor (VEGF), and Fas; (b) cell proliferation curve of primary hepatocytes ($n = 6$), $^*P < 0.05$; (○), WT; (□), TG; (▲), WT+EGF. (c) terminal deoxynucleotidyl transferase-mediated deoxyuridine triphosphate biotin nick end labeling (TUNEL) assay of primary hepatocytes; (d) TUNEL-positive cell counts of primary hepatocytes (per ×200 high-power field). $^*P < 0.05$ in comparison to the WT hepatocytes. TG, transgenic hepatocytes; WT, wild-type hepatocytes.

Journal of Gastroenterology and Hepatology 23 (2008) 260–266 © 2007 The Authors
Journal compilation © 2007 Journal of Gastroenterology and Hepatology Foundation and Blackwell Publishing Asia Pty Ltd

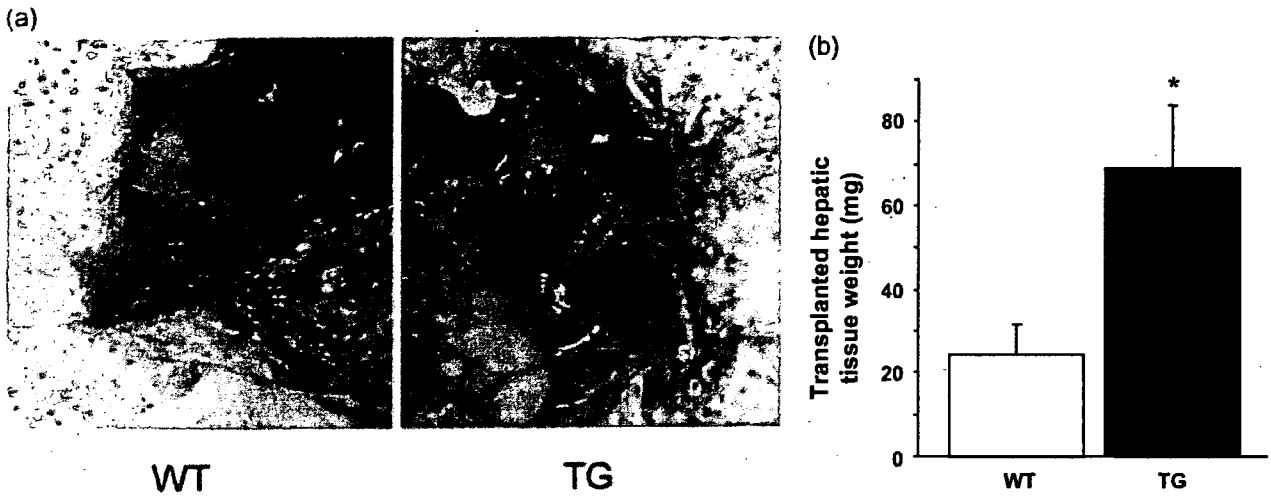

Figure 2 (a) Macroscopic findings of intraperitoneal transplanted hepatic tissue (arrow heads); (b) comparison of the transplanted hepatic tissue weight ($n = 5$); $^*P < 0.05$. TG, transgenic hepatocytes; WT, wild-type hepatocytes.

Proliferation of hepatocytes

The TG hepatocytes increased from day to day; however, the number of WT hepatocytes decreased by 50% after 5 days (Fig. 1b). Furthermore, the WT hepatocytes with EGF (50 ng/mL) increased in a manner similar to that in the TG hepatocytes. This result suggested that the cell proliferation effect of the TGF-α transgene was comparable to the effect of 50 ng/mL EGF.

Anti-Fas antibodies induced apoptosis in the primary hepatocytes

We evaluated the apoptotic cells with TUNEL assay. The number of TUNEL-positive cells in the WT hepatocytes was significantly higher than that of the TG hepatocytes. Furthermore, the resistance to Fas-induced apoptosis of the WT hepatocytes pretreated with 1 μg/mL EGF was almost equal to of the resistance observed in the TG hepatocytes (Fig. 1c,d). However, the levels of Fas expression were similar in both groups of hepatocytes (Fig. 1a).

Macroscopic findings of intraperitoneal hepatic tissues

Two weeks after the transplantation, the intraperitoneally transplanted cells were detected in the peritoneal fatty tissues around the area of aorta and pancreas (Fig. 2a,b). The TG hepatic tissues were clearly larger than the WT hepatic tissues in macro findings (Fig. 2a) and the weight of the TG hepatic tissues were heavier than that of the WT hepatic tissues (Fig. 2b, 68.2 ± 15.3 mg *vs* 24.3 ± 7.48 mg, $P < 0.05$).

Albumin expression in the hepatic tissue

In the microscopic finding, the transplanted cells were detected around the deformed Cytodex3 beads (Fig. 3a). The TG hepatocytes around the Cytodex3 beads were more numerous than the WT hepatocytes. Immunohistochemical staining using anti-albumin antibodies showed that the WT and TG hepatic tissues produced albumin.

CD31 and VEGF expression in the hepatic tissue

The expression of CD31 and VEGF was significantly stronger in the TG hepatic tissues than in the WT hepatic tissues ($n = 5$). This result suggested that the TG hepatocytes induced a greater degree of angiogenesis than the WT hepatocytes during liver reconstitution (Fig. 3b,c).

Discussion

In this study, we demonstrated that the hepatocytes which overexpressed TGF-α were resistant to Fas-induced apoptosis and showed a high degree of proliferative activity after intraperitoneal transplantation. These findings indicated that TGF-α accelerates the growth of transplanted hepatocytes through an autocrine pathway.

Hepatocyte transplantation could be a feasible way to treat acute liver failure due to hepatocyte injury.[4,29] Although hepatocytes have shown almost unlimited proliferative potential in serial transplantation experiments,[30] an obstacle to the successful treatment of liver failure is that the number of hepatocytes that can engraft at one time is often insufficient for treating severe and acute liver failure.[31] The transplantation of a greater number of cells runs the risk of occluding liver circulation.[31,32] Another approach is to modify the donor hepatocytes so that they can more effectively proliferate in the recipient liver.

TGF-α participates in a wide variety of physiological and pathological processes and has been implicated in the process of malignant transformation.[33,34] TGF-α is also a potent mitogen and is a member of the EGF family of peptides.[34–37] TGF-α shares a

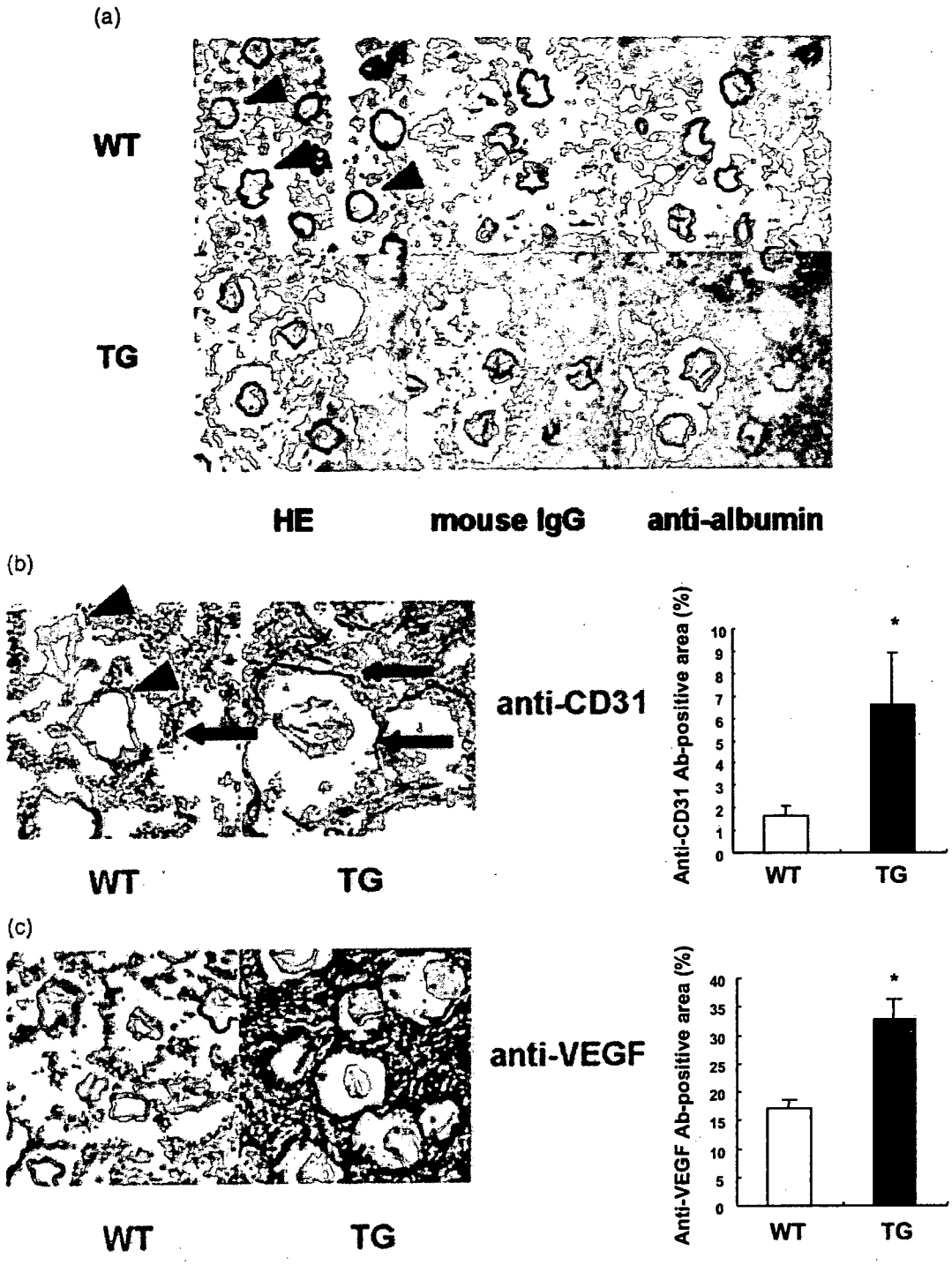

Figure 3 (a) Microscopic findings of transplanted hepatic tissue (left panels: hematoxylin–eosin [HE] stain, center panels: antimouse immunoglobin G stain as the negative control, right panels: antimouse albumin antibodies). Arrow heads show Cytodex3 beads. (b) Immunohistochemistry of CD31 and (c) vascular epidermal growth factor (VEGF). Arrow heads show Cytodex3 beads and arrows show anti-CD31-positive spot. $^*P < 0.05$. TG, transgenic hepatocytes; WT, wild-type hepatocytes.

Journal of Gastroenterology and Hepatology 23 (2008) 260–266

receptor (c-erb B) with EGF and stimulates cellular proliferation by binding to and activating the tyrosine kinase domain of the receptor.[38] We previously demonstrated that mice who overexpressed TGF-α were resistant to liver failure induced by anti-Fas antibodies as well as to ethanol-induced gastric mucosal injury.[13,14] The present study was based on the hypothesis that the hepatocytes derived from TGF-α transgenic mice would have high proliferative activity and resistance to apoptosis. We presumed that these cells would show massive engraftment proliferation after transplantation.

Chen *et al.* reported that the primary hepatocytes stimulated by hepatocyte growth factor (HGF), showed a high level of proliferation,[39] and Kato *et al.* demonstrated that human HGF administration to recipient animals after hepatocyte transplantation accelerated the growth of transplanted tissues.[40] Some recent experiments have involved *in vivo* hepatocyte proliferation using the transgenic mice that overexpressed anti-apoptosis proteins, such as Bcl-2[11] and Bcl-xL[12] or cell cycle regulating factors, such as p27kipl.[10] The results of these studies demonstrated that the donor cells successfully repopulated the host liver after transplantation.

This study is the first report of hepatocyte transplantation performed using hepatocytes overexpressing TGF-α. The transplanted hepatocytes were dissected and examined 2 weeks after transplantation. Wu *et al.* demonstrated that hepatocytes, originated from TGF-α transgenic mice, could be maintained for a long time and established as cell lines.[41,42] Moreover, they reported that this hepatocyte and cell line continued to strongly express transgene hTGFα for several months.

Furthermore, when the hepatocytes' origin from TGF-α transgenic mice was transplanted into the spleen, the expression of TGF-α was detectable for about 2 weeks (Nelson Fausto, pers. comm., 2007)

Moreover, this study demonstrated the continued expression of TGF-α in hepatocytes even after the transplantation.

Ajioka *et al.* previously reported that VEGF plasmids transfected into primary hepatocytes increased the proliferation activity in the liver after hepatocyte transplantation.[43] VEGF-transfected hepatocytes formed a large number of colonies and developed a significant vascular network in established tissues in comparison to control tissues.[43] Several reports have shown that TGF-α induces VEGF expression.[44,45] VEGF mRNA was strongly expressed only in the TG hepatocytes and the expression of VEGF protein in the transplanted TG tissues was strongly detected. These results suggest that the acceleration of angiogenesis followed by VEGF overexpression can cause massive proliferation of transplanted tissues. This idea is consistent with the immunohistological findings of CD31 and VEGF.

However, it has also been reported that the overexpression of TGF-α promotes carcinogenesis.[41,42,46,47] Therefore, the clinical implications of this system are limited to transitory treatment for the activation of hepatocyte proliferation before their transplantation and are carefully reconfirmed by side-effects, including tumorigenesis of the transplanted hepatocytes.

In conclusion, hepatocytes that overexpressed TGF-α showed high proliferative activity and TGF-α accelerated liver tissue reconstitution *in vivo*. These results suggest that hepatocytes that overexpress TGF-α can be used for cell transplantation with the preservation of hepatocyte function. In addition, TGF-α could be a potential target during hepatocyte-based therapies.

Acknowledgments

The authors thank Dr Glenn Merlino (National Institute of Health, Bethesda, MD, USA) for providing the TGF-α transgenic strain MT100, and Dr Nelson Fausto (Department of Pathology, University of Washington, Seattle, WA, USA) for valuable discussion.

References

1 Ohashi K, Park F, Kay MA. Hepatocyte transplantation: clinical and experimental application. *J. Mol. Med.* 2001; **79**: 617–30.
2 Lee LA. Advances in hepatocyte transplantation: a myth becomes reality. *J. Clin. Invest.* 2001; **108**: 367–9.
3 Fox IJ. Transplantation into and inside the liver. *Hepatology* 2002; **36**: 249–51.
4 Strom SC, Chowdhury JR, Fox IJ. Hepatocyte transplantation for the treatment of human disease. *Semin. Liver. Dis* 1999; **19**: 39–48.
5 Isom HC, Tevethia MJ, Kreider JW. Tumorigenicity of simian virus 40-transformed rat hepatocytes. *Cancer Res.* 1981; **41**: 2126–34.
6 Yasui O, Miura N, Terada K, Kawarada Y, Koyama K, Sugiyama T. Isolation of oval cells from Long-Evans Cinnamon rats and their transformation into hepatocytes in vivo in the rat liver. *Hepatology* 1997; **25**: 329–34.
7 Petersen BE, Bowen WC, Patrene KD *et al.* Bone marrow as a potential source of hepatic oval cells. *Science* 1999; **284**: 1168–70.
8 Sandgren EP, Palmiter RD, Heckel JL, Daugherty CC, Brinster RL, Degen JL. Complete hepatic regeneration after somatic deletion of an albumin-plasminogen activator transgene. *Cell* 1991; **66**: 245–56.
9 Overturf K, Al-Dhalimy M, Tanguay R *et al.* Hepatocytes corrected by gene therapy are selected in vivo in a murine model of hereditary tyrosinaemia type I. *Nat. Genet.* 1996; **12**: 266–73.
10 Karnezis AN, Dorokhov M, Grompe M, Zhu L. Loss of p27 (Kip1) enhances the transplantation efficiency of hepatocytes transferred into diseased livers. *J. Clin. Invest.* 2001; **108**: 383–90.
11 Mignon A, Guidotti JE, Mitchell C *et al.* Selective repopulation of normal mouse liver by Fas/CD95-resistant hepatocytes. *Nat. Med.* 1998; **4**: 1185–8.
12 Mitchell C, Mallet VO, Guidotti JE, Goulenok C, Kahn A, Gilgenkrantz H. Liver repopulation by Bcl-x (L) transgenic hepatocytes. *Am. J. Pathol.* 2002; **160**: 31–5.
13 Kanda D, Takagi H, Toyoda M *et al.* Transforming growth factor alpha protects against Fas-mediated liver apoptosis in mice. *FEBS. Lett.* 2002; **519**: 11–15.
14 Kosone T, Takagi H, Kakizaki S *et al.* Integrative roles of transforming growth factor-alpha in the cytoprotection mechanisms of gastric mucosal injury. *BMC Gastroenterol.* 2006; **6**: 22.
15 Takagi H, Jhappan C, Sharp R, Merlino G. Hypertrophic gastropathy resembling Menetrier's disease in transgenic mice overexpressing transforming growth factor alpha in the stomach. *J. Clin. Invest.* 1992; **90**: 1161–7.
16 Takagi H, Sharp R, Hammermeister C *et al.* Molecular and genetic analysis of liver oncogenesis in transforming growth factor alpha transgenic mice. *Cancer Res.* 1992; **52**: 5171–7.
17 Tanaka K, Sato M, Tomita Y, Ichihara A. Biochemical studies on liver functions in primary cultured hepatocytes of adult rats. I. Hormonal effects on cell viability and protein synthesis. *J. Biochem. (Tokyo.)* 1978; **84**: 937–46.
18 Mitaka T, Sattler CA, Sattler GL, Sargent LM, Pitot HC. Multiple cell cycles occur in rat hepatocytes cultured in the presence of nicotinamide and epidermal growth factor. *Hepatology* 1991; **13**: 21–30.
19 Block GD, Locker J, Bowen WC *et al.* Population expansion, clonal growth, and specific differentiation patterns in primary cultures of hepatocytes induced by HGF/SF, EGF and TGF alpha in a

chemically defined (HGM) medium. *J. Cell. Biol.* 1996; **132**: 1133–49.
20 Leung DW, Cachianes G, Kuang WJ, Goeddel DV, Ferrara N. Vascular endothelial growth factor is a secreted angiogenic mitogen. *Science* 1989; **246**: 1306–9.
21 Thomas KA. Vascular endothelial growth factor, a potent and selective angiogenic agent. *J. Biol. Chem.* 1996; **271**: 603–6.
22 Carmeliet P, Ferreira V, Breier G *et al.* Abnormal blood vessel development and lethality in embryos lacking a single VEGF allele. *Nature* 1996; **380**: 435–9.
23 Suda T, Takahashi T, Golstein P, Nagata S. Molecular cloning and expression of the Fas ligand, a novel member of the tumor necrosis factor family. *Cell* 1993; **75**: 1169–78.
24 Hanabuchi S, Koyanagi M, Kawasaki A *et al.* Fas and its ligand in a general mechanism of T-cell-mediated cytotoxicity. *Proc. Natl. Acad. Sci. USA* 1994; **91**: 4930–4.
25 Watanabe Y, Ajioka I, Akaike T. Gene transfection of multicellular spheroid of hepatocytes on an artificial substrate. *Cytotechnical* 1998; **26**: 65–78.
26 Demetriou AA, Levenson SM, Novikoff PM *et al.* Survival, organization, and function of microcarrier-attached hepatocytes transplanted in rats. *Proc. Natl. Acad. Sci. USA* 1986; **83**: 7475–9.
27 Vecchi A, Garlanda C, Lampugnani MG *et al.* Monoclonal antibodies specific for endothelial cells of mouse blood vessels. Their application in the identification of adult and embryonic endothelium. *Eur. J. Cell. Biol.* 1994; **63**: 247–54.
28 Carlos TM, Harlan JM. Leukocyte-endothelial adhesion molecules. *Blood* 1994; **84**: 2068–101.
29 Gupta S, Gorla GR, Irani AN. Hepatocyte transplantation: emerging insights into mechanisms of liver repopulation and their relevance to potential therapies. *J. Hepatol.* 1999; **30**: 162–70.
30 Overturf K, al-Dhalimy M, Ou CN, Finegold M, Grompe M. Serial transplantation reveals the stem-cell-like regenerative potential of adult mouse hepatocytes. *Am. J. Pathol.* 1997; **151**: 1273–80.
31 Braun KM, Degen JL, Sandgren EP. Hepatocyte transplantation in a model of toxin-induced liver disease: variable therapeutic effect during replacement of damaged parenchyma by donor cells. *Nat. Med.* 2000; **6**: 320–6.
32 Groth CG, Arborgh B, Bjorken C, Sundberg B, Lundgren G. Correction of hyperbilirubinemia in the glucuronyltransferase-deficient rat by intraportal hepatocyte transplantation. *Transplant. Proc.* 1977; **9**: 313–16.
33 Derynck R, Goeddel DV, Ullrich A *et al.* Synthesis of messenger RNAs for transforming growth factors alpha and beta and the epidermal growth factor receptor by human tumors. *Cancer Res.* 1987; **47**: 707–12.
34 Salomon DS, Kim N, Saeki T, Ciardiello F. Transforming growth factor-alpha: an oncodevelopmental growth factor. *Cancer Cells* 1990; **2**: 389–97.
35 Carpenter G, Cohen S. Epidermal growth factor. *J. Biol. Chem.* 1990; **265**: 7709–12.
36 Marquardt H, Hunkapiller MW, Hood LE, Todaro GJ. Rat transforming growth factor type 1: structure and relation to epidermal growth factor. *Science* 1984; **223**: 1079–82.
37 Todaro GJ, Rose TM, Spooner CE, Shoyab M, Plowman GD. Cellular and viral ligands that interact with the EGF receptor. *Semin. Cancer Biol.* 1990; **1**: 257–63.
38 Merlino GT. Epidermal growth factor receptor regulation and function. *Semin. Cancer Biol.* 1990; **1**: 277–84.
39 Chen Y, Kobayashi N, Suzuki S *et al.* Transplantation of human hepatocytes cultured with deleted variant of hepatocyte growth factor prolongs the survival of mice with acute liver failure. *Transplantation* 2005; **79**: 1378–85.
40 Kato K, Onodera K, Sawa M *et al.* Effect of hepatocyte growth factor on the proliferation of intrasplenically transplanted hepatocytes in rats. *Biochem. Biophys. Res. Commun.* 1996; **222**: 101–6.
41 Wu JC, Merlino G, Fausto N. Establishment and characterization of differentiated, nontransformed hepatocyte cell lines derived from mice transgenic for transforming growth factor alpha. *Proc. Natl. Acad. Sci. USA* 1994; **91**: 674–8.
42 Wu JC, Merlino G, Cveklova K, Mosinger B Jr, Fausto N. Autonomous growth in serum-free medium and production of hepatocellular carcinomas by differentiated hepatocyte lines that overexpress transforming growth factor alpha 1. *Cancer Res.* 1994; **54**: 5964–73.
43 Ajioka I, Akaike T, Watanabe Y. Expression of vascular endothelial growth factor promotes colonization, vascularization, and growth of transplanted hepatic tissues in the mouse. *Hepatology* 1999; **29**: 396–402.
44 Gille J, Swerlick RA, Caughman SW. Transforming growth factor-alpha-induced transcriptional activation of the vascular permeability factor (VPF/VEGF) gene requires AP-2-dependent DNA binding and transactivation. *EMBO J.* 1997; **16**: 750–9.
45 Maity A, Pore N, Lee J, Solomon D, O'Rourke DM. Epidermal growth factor receptor transcriptionally up-regulates vascular endothelial growth factor expression in human glioblastoma cells via a pathway involving phosphatidylinositol 3'-kinase and distinct from that induced by hypoxia. *Cancer Res.* 2000; **60**: 5879–86.
46 Jhappan C, Stahle C, Harkins RN, Fausto N, Smith GH, Merlino GT. TGF alpha overexpression in transgenic mice induces liver neoplasia and abnormal development of the mammary gland and pancreas. *Cell* 1990; **61**: 1137–46.
47 Lee GH, Merlino G, Fausto N. Development of liver tumors in transforming growth factor alpha transgenic mice. *Cancer Res.* 1992; **52**: 5162–70.

Primary liver cancers with nonalcoholic steatohepatitis

Hiroaki Hashizume[a], Ken Sato[a], Hitoshi Takagi[a], Tomoyuki Hirokawa[a], Akira Kojima[a], Naondo Sohara[a], Satoru Kakizaki[a], Yasushi Mochida[b], Tatsuo Shimura[b], Yutaka Sunose[c], Susumu Ohwada[c] and Masatomo Mori[a]

Nine patients with hepatocellular carcinoma (HCC) in nonalcoholic steatohepatitis (NASH) (six men and three women, median age 71.5 years) and one patient with intrahepatic cholangiocarcinoma (ICC), a 50-year-old man, in NASH are described. Most patients were associated with obesity, diabetes, hypertension, hypercholesterolemia, or hypertriglyceridemia. Seven patients showed insulin resistance and hyperinsulinemia. All patients except one met the criteria for metabolic syndrome. An HCC or ICC diagnosis was confirmed by tumor biopsy, surgery or autopsy except in two patients, who were diagnosed by computed tomography or hepatic angiography. The underlying liver disease was liver cirrhosis in six patients and chronic liver disease including mild hepatic fibrosis in four patients. The treatment of liver cancers consisted of surgery, radio-frequency ablation (RFA), transcatheter arterial embolization and transcatheter arterial infusion. Although the follow-up period was relatively short (median 27.5 months, average 32.1 months), all postoperative and post-RFA patients have not had a recurrence of HCC to date, except for one patient who had a palliative operation with intra-arterial infusion of anticancer drugs through an implanted reservoir port. Older age and liver cirrhosis are considered risk factors for HCC in NASH, and regular screening of these patients is necessary. Diabetes may contribute to the development of ICC in NASH. Curative therapy (surgery or RFA) and weight loss by the active therapeutic intervention (nutritional care and exercise therapy) after curative therapy may help us improve the prognosis of HCC in NASH. *Eur J Gastroenterol Hepatol* **19:827–834 © 2007 Wolters Kluwer Health | Lippincott Williams & Wilkins.**

European Journal of Gastroenterology & Hepatology 2007, 19:827–834

Keywords: hepatocellular carcinoma, intrahepatic cholangiocarcinoma, liver cirrhosis, nonalcoholic steatohepatitis

Departments of [a]Medicine and Molecular Science, [b]General Surgical Science and [c]Thoracic Visceral Organ Surgery, Gunma University Graduate School of Medicine, Maebashi, Gunma, Japan

Correspondence to Ken Sato, MD, PhD, Department of Medicine and Molecular Science, Gunma University Graduate School of Medicine, 3-39-15 Showa, Maebashi, Gunma 371-8511, Japan
Tel: +81 27 220 8127; fax: +81 27 220 8136;
e-mail: satoken@showa.gunma-u.ac.jp

Received 4 February 2007 **Accepted** 10 May 2007

Introduction

Nonalcoholic steatohepatitis (NASH) is a chronic liver disease characterized by the histological features of steatohepatitis in the absence of alcohol consumption. The natural history and prognosis of NASH are unknown because prospective cohort studies in NASH are limited [1,2]. The results of the previous studies, however, suggest that NASH may progress to fibrosis, cirrhosis, and eventually hepatocellular carcinoma (HCC) [1–7].

The recognition of NASH is more widespread as reports of HCC in NASH have increased. The number of case reports is, however, limited and most of them are single or two case-series studies. Notably, there is no report of a case of NASH with intrahepatic cholangiocarcinoma (ICC) without HCC to date. Herein, we describe a large case series of nine patients with NASH and HCC, one patient with NASH and ICC, and review literature detailing clinicopathological features, therapy, and prognosis of HCC in NASH.

0954-691X

Materials and methods

Patients

From 2000 to 2005, we treated 1310 patients with primary liver cancer at Gunma University Graduate School of Medicine and affiliated hospitals. In this group, 34 patients had cryptogenic cirrhosis with HCC or ICC. Of these, 10 patients were diagnosed with pathologically confirmed NASH.

Diagnostic criteria

NASH was diagnosed based on the following criteria: (i) a weekly intake of less than 20 g of ethanol without a history of heavy alcohol consumption; (ii) steatosis (fat in > 10% of hepatocytes), ballooning degeneration, pericellular fibrosis, and perivenular fibrosis confirmed by liver biopsy specimens or surgically removed specimens; (iii) exclusion of other liver diseases such as primary biliary cirrhosis, autoimmune hepatitis, Wilson's disease, hemochromatosis, and drug-induced hepatitis; (iv) absence of serologic or clinical evidence of ongoing hepatitis B (HBV) or hepatitis C (HCV) viral infection. The

presence of obesity was defined as a body mass index (BMI) > 25 kg/m^2 based on the criteria of the Japanese Ministry of Public Welfare.

Laboratory assessments

Laboratory assessments included tests for hepatitis B surface antigen, hepatitis B surface antibody, hepatitis B core antibody, HCV antibody by third generation, anti-nuclear antibody, α-fetoprotein (AFP), and protein induced by vitamin K absence-II (PIVKA-II). Aminotransferase and other routine tests [including fasting blood sugar, fasting serous insulin, and the homeostasis model assessment index (HOMA-IR)], as well as AFP and PIVKA-II testing, were done before liver biopsy or surgery.

Imaging studies

We studied all patients by ultrasonography (US), computed tomography (CT), and selective arteriography. CT hepatic angiography (CTHA) and CT during arterial portography (CTAP) were performed in five patients. HCC was diagnosed by the above imaging studies and confirmed via pathological examination, except in two patients.

Liver histology

All liver specimens were examined using the following stains: hematoxylin–eosin, Azan–Mallory, and silver reticulin. Two independent pathologists carried out the assessment without knowledge of each patient's clinical and biochemical data. Fibrosis was scored using a five-grade scale: F0, normal connective tissue; F1, pericellular or perivenular fibrosis in zone 3; F2, pericellular or perivenular fibrosis confined to zones 3 and 2 with or without periportal fibrosis; F3, bridging or septal fibrosis; F4, cirrhosis [8]. After evaluation of ballooning degeneration, Mallory bodies, disarray of hepatocytes, lobular inflammation, focal necrosis, and lipogranulomas, we constructed a grading scale, which was characterized by mild, moderate, or severe inflammation on the basis of a pathologist's overall impression. The grade of tumor differentiation was assessed to be well differentiated, moderately differentiated, or poorly differentiated.

Results

A summary of our 10 cases with NASH and HCC or ICC is shown in Table 1. Four patients (cases 3, 4, 9, and 10) were not accompanied by liver cirrhosis. Case 10 is the

Table 1 Clinical features of cases with primary liver tumors in NASH

Case	1	2	3	4	5	6	7	8	9	10[a]
Age	74	45	56	82	77	75	71	63	72	50
Sex	Male	Male	Male	Female	Male	Male	Female	Female	Male	Male
BMI (kg/m^2)	24.7	29.4	32.2	26.1	29.7	24.3	25	30	25	31
HL (age at Dx)	59	–	51	67	63	65	60	53	66	43
HT (age at Dx)	59	–	51	68	63	65	60	–	50	–
DM (age at Dx)	59	43	51	–	63	–	67	53	50	43
History of smoking	–	+	–	–	–	–	–	–	–	–
History of blood transfusion	–	–	–	–	–	–	–	–	–	+
Age at onset of abnormal LFT	59	43	54	67	74	65	53	60	70	43
Age at Dx of NASH	74	45	54	82	77	75	67	63	72	50
AST (IU/l)	66	34	35	48	46	66	36	33	41	18
ALT (IU/l)	66	29	22	40	50	59	31	22	46	31
γ-GTP (IU/l)	259	303	34	29	282	445	66	35	152	168
Total bilirubin (mg/dl)	0.6	1.8	0.5	0.4	1.2	0.8	1	0.6	0.55	0.5
Ferritin (ng/ml)	217.1	207.6	150.9	42.8	39	50.5	109.1	67	129.6	370
HOMA-IR	36.2	5.36	4.47	4.6	5.75	3.67	13.5	1.71	1.89	1.76
IRI (μU/ml)	95.7	22.4	13.2	19.2	20.6	16.5	39.2	7.8	7.1	5.4
Varix	–	–	–	–	–	–	+	+	–	–
Ascites	–	+	–	–	–	–	+	–	–	–
AFP (ng/ml)	20.3	175	1195	193.9	17	8.9	31	7	6	3
PIVKA-II (AU/ml)	23	52	74	86	720	16	20	50	1550	40
Location of cancer	S5	S2	S5/8,S6	S4	M	S6	S4	S2	S8	M
Size of cancer (mm)	24	35	70,15	30	30 (max)	30	20	15	40	60 (max)
HBs-Ag	–	–	–	–	–	–	–	–	–	–
Anti-HBc	+	–	–	–	–	–	–	–	–	–
Anti-HCV	–	–	–	–	–	–	–	–	–	–
Age at Dx of HCC or ICC	74	45	54	82	77	75	67	63	72	50
Child–Pugh score at Dx of HCC or ICC	A	B	A	A	A	A	B	A	A	A
ICGR15	NA	16	NA	3.5	16	19.4	38	19.3	NA	9
Underlying liver disease	LC	LC	Non-LC	Non-LC	LC	LC	LC	LC	Non-LC	Non-LC
Tx	Ope	Ope	Ope + RC	Ope	TAE	Ope	RFA	RFA	Ope	TAI
Date of operation	2/23/2004	1/27/2005	11/27/2003	1/21/2005	–	2/5/2005	11/26/2001	6/9/2005	9/3/2002	–
Stage	II	II	IVa	Stage IIIa	IVa	II	I	I	II	IVb

AFP, α-fetoprotein; ALT, alanine aminotransferase; AST, aspartate aminotransferase; BMI, body mass index; DM, diabetes mellitus; Dx, diagnosis; γGTP, γ-glutamyl transpeptidase; HCC, hepatocellular carcinoma; HL, hyperlipidemia; HOMA-IR, homeostasis model assessment-insulin resistance; HT, hypertension; ICC, intracholangiocellular carcinoma; ICGR15, indocyanine green retention rate; IRI, immunoreactive insulin; LC, liver cirrhosis; LFT, liver function test; M, multiple; max, maximum; NA, not applicable; NASH, nonalcoholic steatohepatitis; non-LC, noncirrhotic liver; Ope, operation; PIVKA-II, protein induced by vitamin K absence-II; RC, reservoir chemotherapy; RFA, radio-frequency ablation; S, segment; TAE, transcatheter arterial embolization; TAI, transcatheter arterial infusion; Tx, treatment.
[a]ICC.

first reported patient of ICC accompanied by histologically proven NASH.

Case 1

From 1988, he has received treatment at our hospital for high blood pressure, diabetes, and nonalcoholic fatty liver disease (NAFLD). His diabetes had been controlled with diet and his hypertension was treated with a calcium blocker and β-blocker. He had received an abdominal echo check, biannually. At the age of 74 years, an abdominal US in December 2003 showed a hepatic tumor in segment 5; the lesion measured 2.4 cm in diameter. Hepatic arteriography, CTHA, and CTAP revealed the characteristics of an HCC. We found no evidence of metastases or vascular invasion. He underwent surgery. The macroscopic finding of the resected liver was micronodular cirrhosis, and an encapsulated white tumor was observed in the cirrhotic liver. The resected specimen showed a well to moderately differentiated HCC with steatosis and Mallory bodies. The noncancerous areas of the resected specimen showed cirrhosis with macrovesicular/microvesicular steatosis, intralobular infiltration of inflammatory cells, ballooned hepatocytes, pericellular fibrosis, and Mallory bodies. Thirty-three months after surgery, there was no HCC recurrence.

Case 2

A 45-year-old obese man was referred to our hospital for the treatment of obstructive jaundice. He had a 3-year history of insulin-independent diabetes mellitus, fatty liver, and mildly increased transaminase levels. The diabetes was controlled by diet and exercise. US and CT revealed an enhanced 2.5 cm tumor at the porta hepatis, which compressed a bile duct and subsequently caused obstructive jaundice. Endoscopic retrograde cholangiopancreatography showed that the upper bile duct was blocked by tumor. He underwent surgery. The resected tumor displayed features of a moderately differentiated HCC with trabecular patterns, and the tumor cells also contained some fat. The noncancerous areas of the resected specimen showed cirrhosis and mild fatty change, intralobular infiltration of inflammatory cells, ballooned hepatocytes, pericellular and perivenular fibrosis. No recurrence of HCC has been detected in the 22 months postsurgery.

Case 3

A 54-year-old obese man was referred to our hospital for the treatment of HCC detected by CT in October 2003. About 4 years before, he had insulin-independent diabetes mellitus, hypertension, hypercholesterolemia, hypertriglyceridemia, slightly high aminotransferase values, and so-called NAFLD. Since then, he was treated with oral antihyperglycemic agents and an angiotensin II receptor blocker. US, hepatic arteriography, CTHA, and CTAP revealed a main tumor in segment 5/8; the lesion measured 7 cm in diameter and a daughter tumor was found in segment 6; the lesion measured 1.5 cm in diameter, but there were no signs of liver cirrhosis. Serum AFP and PIVKA-II values increased. He underwent anterior segmentectomy. The resected tumor had features of a poorly differentiated HCC. The vessel involvement was diagnosed postoperatively. The noncancerous areas of the resected specimen showed noncirrhosis with macrovesicular/microvesicular steatosis, intralobular infiltration of inflammatory cells, ballooned hepatocytes, and pericellular fibrosis. As the surgical margin of HCC was small, we could not judge whether HCC was completely resected. Thus, he postoperatively underwent continuous intraarterial infusion of 5-fluorouracil through an implanted reservoir port and interferon subcutaneously. The treatment was repeated every 4 weeks with a maximum of four cycles. After four cycles, serum AFP levels decreased from 1195 ng/ml to the normal level and CT showed no HCC recurrence. He has been well and continued to receive interferon and 5-fluorouracil at the outpatient clinic for the last 13 months.

Case 4

An 82-year-old obese woman was referred to our hospital for the treatment of an HCC. She had been diagnosed with obesity, diabetes type 2, hypercholesterolemia, hypertriglyceridemia, and NAFLD at the age of 67 years. The diabetes was controlled by diet without medications. Using US, hepatic arteriography, CTHA, and CTAP, we confirmed the presence of HCC in segment 4; the lesion measured 4 cm in diameter. We found no evidence of vascular invasion or metastases. As her general condition was good, she underwent surgery. The resected tumor had features of a moderately differentiated HCC (Fig. 1a). The noncancerous areas of the resected specimen showed noncirrhosis with macrovesicular/microvesicular steatosis, intralobular infiltration of inflammatory cells, ballooned hepatocytes, pericellular fibrosis, and Mallory bodies (Fig. 1b–d). She has been cancer-free for 22 months after the operation.

Case 5

A 77-year-old man was treated with a cholinesterase inhibitor for myasthenia gravis that had been discovered at the age of 73 years. He also had a 14-year history of obesity (BMI = 29.7); diabetes mellitus, hypertension, hypercholesterolemia, hypertriglyceridemia, and NAFLD. His aminotransferase levels remained within two to three times the upper limit of normal. Liver biopsy was performed at the age of 74 years. A biopsy sample showed cirrhosis with moderate fatty change, intralobular infiltration of inflammatory cells, ballooned hepatocytes, pericellular and perivenular fibrosis. During follow-up, US studies revealed the presence of multiple hypoechoic tumors. Using CT and hepatic arteriography, the tumors did not show early enhancement and the images are

Fig. 1

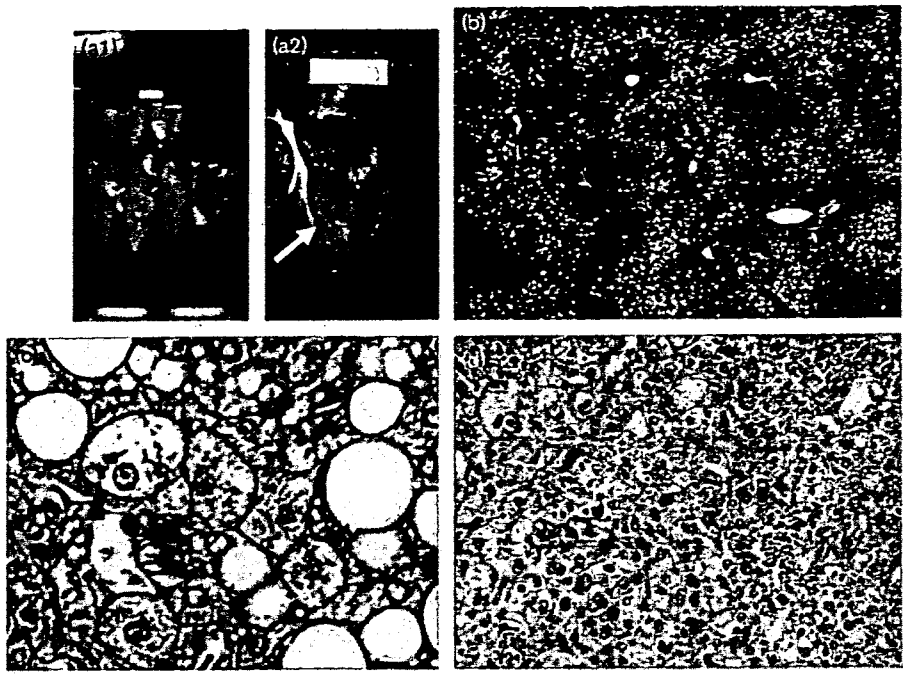

(a) (1) Resected liver specimens. (2) Magnification of the resected specimen shows a well-demarcated HCC (arrow), measuring 3.0 cm in diameter. (b) Microscopic features of the noncancerous area of the surgical specimen. Microvesicular and macrovesicular fatty changes in zone 3 (H&E, ×40). (c) Steatohepatitis with ballooning degeneration of hepatocytes and Mallory bodies (arrowhead) (H&E, × 400). (d) The tumor specimen shows atypical hepatocytes with a high nuclear/cytoplasmic (N/C) ratio and increased cellularity (H&E, × 200). H&E, hematoxylin–eosin staining.

atypical of HCCs. He was treated with transcatheter arterial embolization (TAE), but the effect of TAE was insufficient. After 11 months, he died of acute obstructive suppurative cholangitis caused by the common bile duct stones. At autopsy, the tumor had features of moderately differentiated HCC with trabecular patterns. The noncancerous areas showed cirrhosis with macrovesicular steatosis, intralobular infiltration of inflammatory cells, ballooned hepatocytes, pericellular fibrosis, and Mallory bodies.

Case 6

He was diagnosed with hypertension, hypercholesterolemia, hypertriglyceridemia, and NAFLD in 1995. After about 10 years, a liver neoplasm was discovered on abdominal echo. CT revealed a 3.0 cm HCC in segment 6. He underwent three liver biopsies (Fig. 2a–f) until the cancer was discovered. These biopsy specimens showed that liver fibrosis progressively worsened each time. He underwent surgery. The resected tumor had features of moderately differentiated HCC (Fig. 2a). The noncancerous areas of the resected specimen showed cirrhosis with macrovesicular/microvesicular steatosis, intralobular infiltration of inflammatory cells, ballooned hepatocytes, pericellular fibrosis, and Mallory bodies. He has been well since surgery.

Case 7

She had been diagnosed with obesity, hypercholesterolemia, hypertriglyceridemia, and NAFLD at the age of 60 years. She developed diabetes at the age of 66 years. About a year later, an abdominal echo described that her liver had a neoplasm. CT revealed a 2.0 cm HCC in segment 4. After liver biopsy was performed, she underwent radio-frequency ablation (RFA) in November 2001. Biopsy sample showed cirrhosis with moderate fatty change, intralobular infiltration of inflammatory cells, ballooned hepatocytes, and pericellular and perivenular fibrosis. So far, she has had no recurrence of HCC after RFA.

Case 8

She had been diagnosed with diabetes mellitus, obesity, hypertriglyceridemia, and NAFLD at the age of 53 years. When she was 61, esophageal varices were detected via an upper-gastrointestinal-tract endoscope from another hospital. She was introduced to our hospital and her esophageal varices were treated by endoscopic variceal ligation. US and CT revealed fatty liver, cirrhosis, and splenomegaly, although a liver biopsy was not performed. Since then, she has regularly undergone CT or US. Two years later, the CT detected a tumor in segment 2; the lesion measured 1.5 cm in diameter. Liver biopsy was

Fig. 2

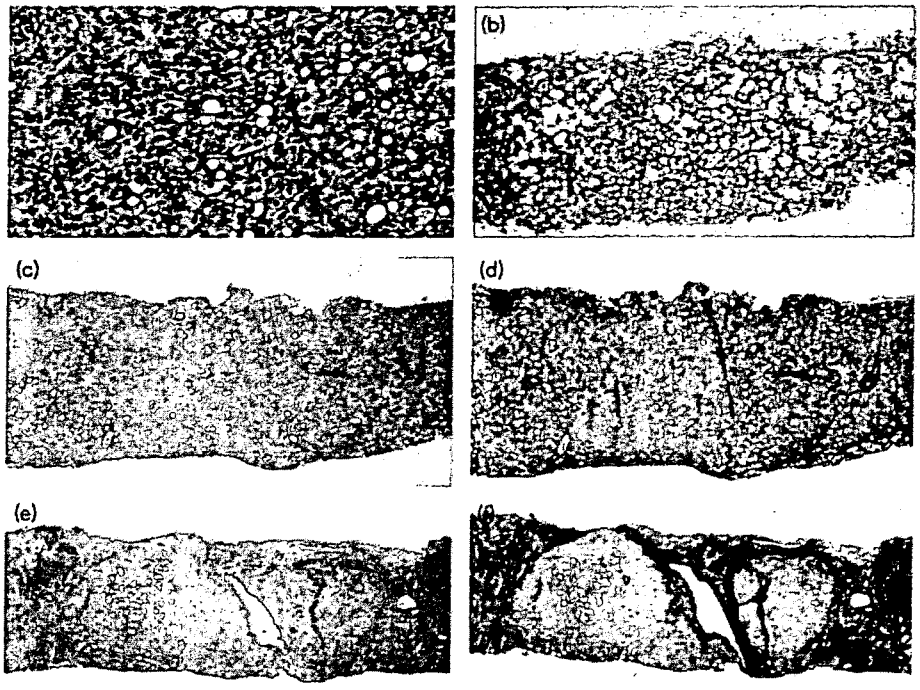

(a) The tumor specimen on February 2005 shows atypical hepatocytes with a high nuclear/cytoplasmic (N/C) ratio and increased cellularity. (b) First biopsy on August 2002 shows steatohepatitis but no fibrosis. (c, d) Second biopsy on January 2003 shows decreased steatosis and increased fibrosis. (e, f) Third biopsy on February 2005 shows liver cirrhosis and more decreased steatosis. (a) H&E, ×200; (b, c, e) H&E, ×40; (d, f) Azan–Mallory, ×40. H&E, hematoxylin–eosin staining.

performed and the biopsy samples showed cirrhosis with fatty change, intralobular infiltration of inflammatory cells, ballooned hepatocytes, and pericellular and perivenular fibrosis. After confirming that the abdominal angiography showed a tumor stain, she received RFA. So far, she has had no recurrence of HCC after RFA.

Case 9

At the age of 48 years, he was diagnosed with obesity and diabetes. Thereafter, however, he had never visited the office. He was diagnosed with hypertension and hypertriglyceridemia during the medical checkup at 64 years of age. When aged 67 years, he underwent percutaneous transluminal coronary angioplasty based on the diagnosis of angina pectoris. Since then, he has been regularly followed at the division of cardiovascular disease. About 4 years later, the abdominal echo checkup revealed a 4 cm tumor in segment 8. CT, MRI, and angiography showed HCC and he underwent surgery. Fifty months after surgery, no HCC recurrence has been detected.

Case 10

A 50-year-old obese man with insulin-independent diabetes mellitus, hypertension, hypercholesterolemia, and hypertriglyceridemia had liver enzyme alterations, and NAFLD was detected 8 years earlier. For about 1 year since October 2003, he had not received regular outpatient treatment. Then, he visited the affiliated hospital because of right upper abdominal pain. CT revealed multiple nonenhanced tumors and fatty liver with no signs of liver cirrhosis. The image-guided biopsy was reported as multifocal diffuse macrovesicular/microvesicular steatosis with focal areas of steatohepatitis and pericellular and perivenular fibrosis, and poorly differentiated adenocarcinoma with tubular proliferation. In the immunostaining, cytokeratin 7 (CK7) was positive. Therefore, we diagnosed NASH with ICC. He was treated by transcatheter arterial infusion. After 1 month, he died of ICC and liver failure in April 2004. The autopsy (Fig. 3a–d) confirmed that the tumor was CK7-positive and a poorly differentiated cholangiocarcinoma. The noncancerous areas showed noncirrhosis with macrovesicular/microvesicular steatosis, intralobular infiltration of inflammatory cells, ballooned hepatocytes, and pericellular fibrosis.

Discussion

We presented nine NASH-related HCC cases (six men and three women) and the first reported case of NASH-related ICC without HCC in noncirrhotic liver. Four patients were not accompanied by liver cirrhosis. The median age at diagnosis of HCC in our patients was 71.5

Fig. 3

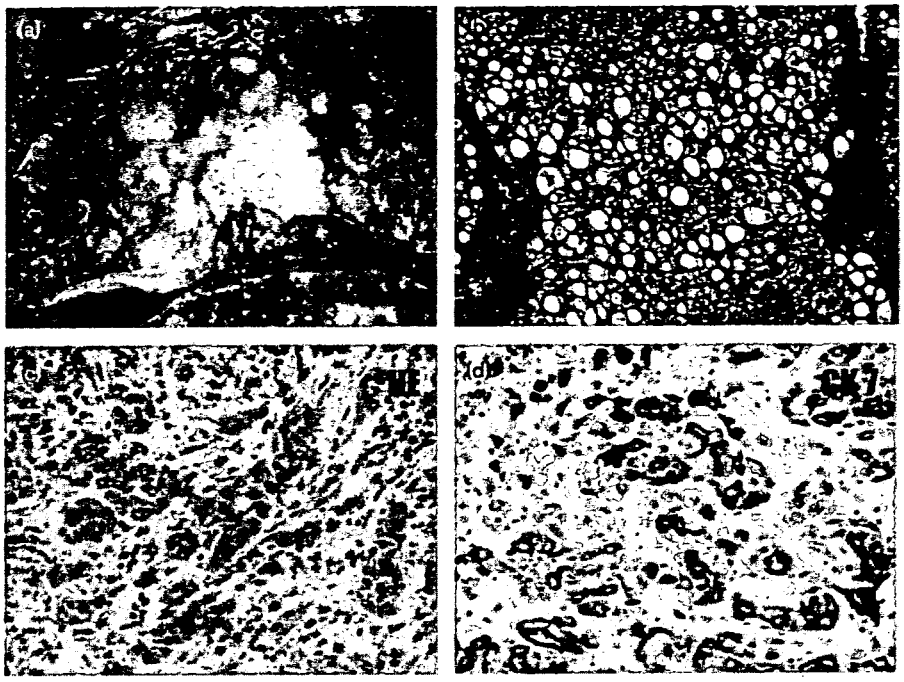

(a) Autopsy specimen with multiple tumors. (b) Microscopic features of noncancerous area show steatohepatitis with ballooning degeneration of hepatocytes in zone 3. (c, d) The tumor specimen shows atypical hepatocytes with a high nuclear/cytoplasmic (N/C) ratio, and cytokeratin 7 (CK 7) staining is positive. (b) H&E, ×40; (c) H&E, ×400; (d) CK7, ×400. H&E, hematoxylin–eosin staining.

years. All patients had been diagnosed with diabetes, hypertension, or hypertriglyceridemia. Aside from Case 2, our cases met diagnostic criteria for metabolic syndrome. Seven patients showed insulin resistance, which was evaluated based on homeostasis model assessment-insulin resistance (≥ 2.0). The treatment of liver cancer consisted of surgery (six patients), RFA (two patients), TAE (one patient) and transcatheter arterial infusion (one patient). Although the observation periods are relatively short in our study, there was no relapse after curative therapies were implemented (surgery or RFA).

The most important causative factors of HCC were HBV and HCV infection. In our study, Case 1 was positive for hepatitis B core antibody, but the liver failed to show any morphological features of chronic hepatitis B. We did not detect HBV-DNA in serum and liver tissue. Hence, we concluded that NASH, not the earlier infection with hepatitis B, played an essential role in the development of HCC. In addition, NASH inducing drugs were not administered throughout or before the clinical course.

HCC is reported to be a late complication in the natural history of NASH [2–7]. Several reports [4,7,9] have described the development of HCC in aged patients with NASH or obesity-related cryptogenic cirrhosis. Bugianesi *et al.* [4] reported that patients with cryptogenic cirrhosis and HCC were older than other control groups (alcohol-related HCC, HBV-related HCC, and HCV-related HCC; median age, 69 versus 64 years). Ratziu *et al.* [7] found that the mean age of HCC detection in overweight patients with cryptogenic cirrhosis was 66.8 years. Hashimoto *et al.* [9] compared the characteristics of alcoholic liver disease and NASH patients with HCC and reported the median age at 65 years in the alcoholic liver disease-HCC group and 68 years in the NASH group. Table 2 summarizes the clinical features and histological characteristics of the previous patients [2,9–18]. The median age of our patients is 71.5 years. Given all the cases, the patient's age was greater than 60 years in 29 out of 36 cases (81%). On the other hand, cirrhosis itself is recognized as a common factor promoting HCC. In 24 out of 35 patients (69%), NASH-related HCC was accompanied by liver cirrhosis. To date, six patients with NASH-related HCC in noncirrhotic liver were reported [9,10,16–18]. Our three patients (cases 3, 4 and 9) confirmed that HCC developed in noncirrhotic NASH liver. Aside from the two patients (including our case 3) of noncirrhotic liver [10], all patients were older than 60. Thus, our findings were consistent with previous studies showing that age [5,9] and advanced hepatic fibrosis [5,9,18] or cirrhosis [3,14,15] are risk factors for HCC development. Thus, aging and cirrhosis were considered to be risk factors for HCC development in NASH. Therefore, we concluded that regular screening, including tumor markers and imaging studies, is necessary to

Table 2 Clinicopathologic features of cases with NASH and HCC in previous reports

Case	Author	Age	Sex	Background disease	HCC histology	Liver histology	Treatment	Outcome
1	Powell *et al.*	57	F	DM	NA	LC	Operation	Dead
2	Cotrim *et al.*	62	M	OB, DM	NA	LC	PEI	Dead
3	Zen *et al.*	72	F	DM	Wel, Mod	NA	NA	NA
4	Orikasa *et al.*	67	F	DM	Clear cell	LC	Operation	NA
5	Shimada *et al.*	66	F	DM	Mod	LC	Operation	Recurrence
6	Shimada *et al.*	69	F	HT	Wel	LC	TAE	Dead
7	Shimada *et al.*	69	F	OB, DM	NA	LC	TAI	Recurrence
8	Shimada *et al.*	72	M	OB	Wel	LC	TAE, PEI	Recurrence
9	Shimada *et al.*	63	M	OB, HL	Wel	LC	Operation	No recurrence
10	Shimada *et al.*	56	M	DM	Mod	LC	TAE	Dead
11	Hashimoto *et al.*	57	F	DM, HL	NA	LC	NA	NA
12	Hashimoto et al.	68	F	DM	NA	LC	NA	NA
13	Hashimoto *et al.*	71	F	OB, DM, HT	NA	LC	NA	NA
14	Hashimoto *et al.*	79	F	OB, HT	NA	LC	NA	NA
15	Hashimoto *et al.*	59	M	OB, HL	NA	Non-LC	NA	NA
16	Hashimoto *et al.*	65	M	OB, DM	NA	LC	NA	NA
17	Hashimoto *et al.*	68	M	DM	NA	LC	NA	NA
18	Hashimoto *et al.*	71	M	OB, DM	NA	LC	NA	NA
19	Hashimoto *et al.*	89	M	OB	NA	LC	NA	NA
20	Mori *et al.*	76	M	OB, DM	Wel	LC	RFA	No recurrence
21	Cuadrado *et al.*	74	M	OB, DM	Wel	Non-LC	RFA	Recurrence
22	Cuadrado *et al.*	69	M	OB, DM	NA	LC	Transplantation	NA
23	Sato *et al.*	64	M	OB, HL	Mod	Non-LC	NA	Dead
24	Hai *et al.*	72	M	OB, DM, HT, HL	Mod	Non-LC	Operation	NA
25	Hai *et al.*	65	M	OB, DM	Mod	LC	Operation	NA
26	Ichikawa *et al.*	66	F	OB, HT, HL	Mod	Non-LC	Operation	Recurrence
27	Ichikawa *et al.*	60	M	DM	Mix	Non-LC	Operation	No recurrence

DM, diabetes mellitus; F, female; HCC, hepatocellular carcinoma; HL, hyperlipidemia; HT, hypertension; LC, liver cirrhosis; M, male; Mix, combined hepatocellular and intrahepatic cholangiocarcinoma (mixed carcinoma); Mod, moderately differentiated; NA, not applicable; NASH, nonalcoholic steatohepatitis; Non-LC, noncirrhotic liver; OB, obesity; PEI, percutaneous ethanol injection; RC, continuous intra-arterial infusion of anticancer drugs through an implanted reservoir port; RFA, radio-frequency ablation; TAE, transcatheter arterial embolization; TAI, transcatheter arterial infusion; Wel, well differentiated.

detect HCC earlier in NASH patients of older age or those with cirrhosis.

Obesity and diabetes are significantly associated with HCC development [19,20]. Diabetes was found to be a risk factor for HCC independent of age, sex, and race [21]. Obesity and diabetes are major risk factors for NASH [3,22]. Hyperinsulinemia and insulin resistance are associated with obesity and diabetes [23–25]. Exposure to physiological insulin concentrations stimulates the proliferation of human and rat hepatoma cell lines, and chronic hyperinsulinemia and insulin-like growth factor 1 might be involved in hepatocarcinogenesis [21]. When hyperinsulinemia was defined according to our laboratory upper limit normal ($> 10\,\mu U/ml$), most of our patients were consistent with the diagnosis standard of metabolic syndrome and many showed hyperinsulinemia (Table 1). Thus, obesity, diabetes, and hyperinsulinemia may contribute to HCC development in our patients.

Case 10, in which the underlying abnormality was noncirrhotic liver disease, was accompanied by ICC. It is unclear whether ICC was derived from NASH. NASH, incidentally, may be accompanied by ICC. A recent case study [18] has reported that a combination of HCC and ICC developed in NASH. The patient had diabetes. The recent largest population-based case–control study [26] suggested that the following factors were significant risk factors for ICC (i.e. nonspecific cirrhosis and alcoholic liver disease such as chronic noninfectious liver disease; HCV and HIV infection as chronic infectious liver disease; cholangitis, choledocholithiasis, and cholestasis as bile duct disease; diabetes; smoking; a history of inflammatory bowel disease) [26]. Taken together, the presentation of diabetes and NASH may contribute to the development of ICC in Case 10. Prospective studies about the incidence or risk factors of ICC in NASH patients need to be elucidated.

Most of our patients revealed good liver function at HCC diagnosis. Six patients (Cases 1–4, 6 and 9) underwent surgery and two patients (Cases 7 and 8) underwent RFA. No cases of HCC recurrence have been detected. HCC recurrence after operation or RFA, however, was often observed in the previous reports (Table 2). In our study, some experienced weight loss to ideal body weight after operation or RFA by active intervention of nutritional care and exercise therapy for NASH. HCC treatment seems to be a powerful motivator and improves lifestyle. This intervention may contribute to no recurrence rate after curative therapy, although the observation periods are relatively short (17–60 months). Therefore, earlier HCC detection for curative therapy is considered crucial for better prognosis. An earlier diagnosis of HCC in NASH patients, however, appears to be difficult and delayed in comparison with patients with other chronic liver diseases, because the diagnosis of NASH is delayed as a result of the need for liver biopsy in the definitive diagnosis.

In conclusion, older age (especially greater than 60) and liver cirrhosis are considered risk factors for HCC in NASH. Diabetes may contribute to the development of ICC in NASH. As an earlier diagnosis for HCC and curative therapy are crucial for better prognosis, the early and definitive diagnosis of NASH and regular screening of high-risk groups for HCC development is necessary. The active therapeutic intervention may help improve the prognosis after curative therapy. If the criteria for patients screened for HCC, however, were to be applied to every obese, diabetic without cirrhosis greater than 60 years, it would create a cost-effective problem, especially in an obesity epidemic area such as USA. Given that 32 of 36 patients (89%) of NASH-related HCC were reported in Japan, there may be a racial risk of HCC in Japanese. Accumulation of cases of NASH-related HCC, in all the countries of the world, may allow us to refine better the patients who would be screen eligible. In addition, prospective cohort studies assessing the development of primary liver cancers in NASH patients are ongoing in our laboratory.

Acknowledgement

Conflicts of interest – none declared.

References

1 Hui JM, Kench JG, Chitturi S, Sud A, Farrell GC, Byth K, *et al.* Long-term outcomes of cirrhosis in nonalcoholic steatohepatitis compared with hepatitis C. *Hepatology* 2003; **38**:420–427.

2 Powell EE, Cooksley WG, Hanson R, Searle J, Halliday JW, Powell LW. The natural history of nonalcoholic steatohepatitis: a follow-up study of forty-two patients for up to 21 years. *Hepatology* 1990; **11**:74–80.

3 Ludwig J, Viggiano TR, McGill DB, Oh BJ. Nonalcoholic steatohepatitis: Mayo Clinic experiences with a hitherto unnamed disease. *Mayo Clin Proc* 1980; **55**:434–438.

4 Bugianesi E, Leone N, Vanni E, Marchesini G, Brunello F, Carucci P, *et al.* Expanding the natural history of nonalcoholic steatohepatitis: from cryptogenic cirrhosis to hepatocellular carcinoma. *Gastroenterology* 2002; **123**:134–140.

5 Yatsuji S, Hashimoto E, Kaneda H, Taniai M, Takakura M, Tokushige K, *et al.* Characteristic features and risk factors for hepatocellular carcinoma in nonalcoholic steatohepatitis. *Hepatology* 2005; **42 (Suppl 1)**:625A.

6 Hashimoto E, Yatsuji S, Kaneda H, Yoshioka Y, Taniai M, Tokushige K, *et al.* The characteristics and natural history of Japanese patients with nonalcoholic fatty liver disease. *Hepatol Res* 2005; **33**:72–76.

7 Ratziu V, Bonyhay L, Di Martino V, Charlotte F, Cavallaro L, Sayegh-Tainturier MH, *et al.* Survival, liver failure, and hepatocellular carcinoma in obesity-related cryptogenic cirrhosis. *Hepatology* 2002; **35**:1485–1493.

8 Brunt EM, Janney CG, Di Bisceglie AM, Neuschwander-Tetri BA, Bacon BR. Nonalcoholic steatohepatitis: a proposal for grading and staging the histological lesions. *Am J Gastroenterol* 1999; **94**: 2467–2474.

9 Hashimoto E, Taniai M, Kaneda H, Tokushige K, Hasegawa K, Okuda H, *et al.* Comparison of hepatocellular carcinoma patients with alcoholic liver disease and nonalcoholic steatohepatitis. *Alcohol Clin Exp Res* 2004; **28 (8 Suppl, Proc)**:164S–168S.

10 Cuadrado A, Orive A, Garcia-Suarez C, Dominguez A, Fernandez-Escalante JC, Crespo J, *et al.* Non-alcoholic steatohepatitis (NASH) and hepatocellular carcinoma. *Obes Surg* 2005; **15**:442–446.

11 Cotrim HP, Parana R, Braga E, Lyra L. Nonalcoholic steatohepatitis and hepatocellular carcinoma: natural history? *Gastroenterology* 2000; **95**:3018–3019.

12 Zen Y, Katayanagi K, Tsuneyama K, Harada K, Araki I, Nakanuma Y. Hepatocellular carcinoma arising in non-alcoholic steatohepatitis. *Pathol Int* 2001; **51**:127–131.

13 Orikasa H, Ohyama R, Tsuka N, Eyden BP, Yamazaki K. Lipid-rich clear-cell hepatocellular carcinoma arising in non-alcoholic steatohepatitis in a patient with diabetes mellitus. *J Submicrosc Cytol Pathol* 2001; **33**:195–200.

14 Shimada M, Hashimoto E, Taniai M, Hasegawa K, Okuda H, Hayashi N, Takasaki K, Ludwig J. Hepatocellular carcinoma in patients with non-alcoholic steatohepatitis. *J Hepatol* 2002; **37**:154–160.

15 Mori S, Yamasaki T, Sakaida I, Takami T, Sakaguchi E, Kimura T, *et al.* Hepatocellular carcinoma with nonalcoholic steatohepatitis. *J Gastroenterol* 2004; **39**:391–396.

16 Sato K, Ueda Y, Ueno K, Okamoto K, Iizuka H, Katsuda S, *et al.* Hepatocellular carcinoma and nonalcoholic steatohepatitis developing during long-term administration of valproic acid. *Virchows Arch* 2005; **447**:996–999.

17 Hai S, Kubo S, Shuto T, Tanaka H, Takemura S, Yamamoto T, *et al.* Hepatocellular carcinoma arising from nonalcoholic steatohepatitis: report of two cases. *Surg Today* 2006; **36**:390–394.

18 Ichikawa T, Yanagi K, Motoyoshi Y, Hamasaki K, Nakao K, Toriyama K, *et al.* Two cases of non-alcoholic steatohepatitis with development of hepatocellular carcinoma without cirrhosis. *J Gastroenterol Hepatol* 2006; **21**:1865–1866.

19 Calle EE, Rodriguez C, Walker-Thurmond K, Thun MJ. Overweight, obesity, and mortality from cancer in a prospectively studied cohort of U.S. adults. *N Engl J Med* 2003; **348**:1625–1638.

20 Davila JA, Morgan RO, Shaib Y, McGlynn KA, El-Serag HB. Diabetes increases the risk of hepatocellular carcinoma in the United States: a population based case control study. *Gut* 2005; **54**:533–539.

21 Saito K, Inoue S, Saito T, Kiso S, Ito N, Tamura S, *et al.* Augmentation effect of postprandial hyperinsulinaemia on growth of human hepatocellular carcinoma. *Gut* 2002; **51**:100–104.

22 Marchesini G, Bugianesi E, Forlani G, Cerrelli F, Lenzi M, Manini R, *et al.* Nonalcoholic fatty liver, steatohepatitis, and the metabolic syndrome. *Hepatology* 2003; **37**:917–923.

23 Weyer C, Hanson RL, Tataranni PA, Bogardus C, Pratley RE. A high fasting plasma insulin concentration predicts type 2 diabetes independent of insulin resistance: evidence for a pathogenic role of relative hyperinsulinemia. *Diabetes* 2000; **49**:2094–2101.

24 Kahn SE, Hull RL, Utzschneider KM. Mechanisms linking obesity to insulin resistance and type 2 diabetes. *Nature* 2006; **444**:840–846.

25 Koyama K, Chen G, Lee Y, Unger RH. Tissue triglycerides, insulin resistance, and insulin production: implications for hyperinsulinemia of obesity. *Am J Physiol* 1997; **273**:E708–713.

26 Shaib YH, El-Serag HB, Davila JA, Morgan R, McGlynn KA. Risk factors of intrahepatic cholangiocarcinoma in the United States: a case–control study. *Gastroenterology* 2005; **128**:620–626.

Liver International ISSN 1478-3223

BASIC STUDIES

Overexpression of NK2 promotes liver fibrosis in carbon tetrachloride-induced chronic liver injury

Satoshi Hagiwara, Toshiyuki Otsuka, Yuichi Yamazaki, Takashi Kosone, Naondo Sohara, Takeshi Ichikawa, Ken Sato, Satoru Kakizaki, Hitoshi Takagi and Masatomo Mori

Department of Medicine and Molecular Science, Gunma University Graduate School of Medicine, Maebashi, Gunma, Japan

Keywords
hepatocyte growth factor – liver fibrosis – NK2

Correspondence
Toshiyuki Otsuka, MD, PhD, Department of Medicine and Molecular Science, Gunma University Graduate School of Medicine, 3-39-15 Showa-machi, Maebashi, Gunma 371-8511, Japan
Tel: +81 27 220 8127
Fax: +81 27 220 8136
e-mail: tcht-otsuka@tonehoken.or.jp

Received 28 April 2007
accepted 19 September 2007

DOI:10.1111/j.1478-3231.2007.01616.x

Abstract

Background/Aims: Hepatocyte growth factor (HGF) inhibits liver fibrosis induced by carbon tetrachloride (CCl_4) in animal models. NK2 is a natural splice variant of HGF, but its *in vivo* function remains to be elucidated. We investigated the *in vivo* effects of NK2 on CCl_4-induced liver fibrosis. *Methods:* NK2 transgenic mice and wild-type (WT) mice were injected intraperitoneally with CCl_4 twice a week. The extent of hepatic fibrosis was evaluated by Azan–Mallory staining. Expression levels of mRNAs of transforming growth factor-β1 (TGF-β1) and matrix metalloproteinase-13 (MMP-13) were examined by real-time polymerase chain reaction. The protein levels of α-smooth muscle actin (α-SMA), c-Met and its phosphorylation were determined by Western blot analysis. *Results:* Liver fibrosis was significantly more severe in NK2 transgenic mice than in WT mice. CCl_4 administration increased the expression levels of TGF-β1 mRNA and α-SMA protein, and decreased the expression of MMP-13 mRNA in livers of NK2 transgenic mice compared with those of WT mice. c-Met protein expression in the liver was compatible with the degree of fibrosis. As for c-Met activation, no difference was found between NK2 and WT livers. *Conclusion:* Overexpression of NK2 acts as an antagonist of HGF and promotes liver fibrosis in CCl_4-induced chronic liver injury.

Hepatocyte growth factor (HGF), also known as the scatter factor, was originally identified as a potent mitogen for hepatocytes (1–7). HGF is a multifunctional mediator that shows motogenic and morphogenic activities in a variety of cells in addition to mitogenic activity (7). The multitude biological activities of HGF are mediated through c-Met, a transmembrane tyrosine kinase receptor (8, 9). The receptor has two subunits (α and β) and the intracellular domain of the β subunit has tyrosine kinase activity and transduces the effects of HGF (9).

Hepatic stellate cells (HSCs) play a central role in hepatic fibrosis. Quiescent HSCs function as major vitamin A storing cells. However, HSCs are activated or transdifferentiated into myofibroblast-like phenotype in certain pathological conditions such as liver fibrosis and cirrhosis (10). During liver injury, transforming growth factor-β1 (TGF-β1), which is secreted by Kupffer cells, stimulates proliferation and induces activation of HSCs. The activated HSCs, which express α-smooth muscle actin (α-SMA), overexpress TGF-β1. TGF-β1 is involved in the excessive production of extracellular matrix (ECM) components and hepatic fibrosis (11). TGF-β1 is also reported to inhibit the proliferation of rat hepatocytes both *in vitro* and *in vivo* (12, 13). On the other hand, the early phase of liver injury and progression phase of liver fibrosis are characterized by overexpression of matrix metalloproteinases (MMPs), which specifically degrade fibrillar collagen. Recent experimental studies indicated also that HGF inhibits hepatic fibrosis in animal models (14–17). HGF suppresses the activation and proliferation of HSCs and inhibit overexpression of TGF-β1 (14). Moreover, HGF inhibits ECM deposition and reduces the amount of pre-existing ECM constituents including fibrillar collagens through upregulation of MMP-1, which is a member of MMPs family (11). Human MMP-1 is a counter protein of mouse MMP-13.

Hepatocyte growth factor mRNA undergoes alternative splicing to create truncated isoforms including NK2 (18). HGF is a heterodimeric glycoprotein consisting of an α-chain, which has an N domain and four

kringle domains and a β-chain (5). On the other hand, NK2 consists of an N domain and the first two kringle domains of HGF (18). NK2 can bind to c-Met with relatively high affinity and is considered an HGF antagonist for a variety of biological activities *in vitro* (19–22). In a series of studies, we have demonstrated previously that NK2 antagonizes HGF actions in cellular proliferation, protection against carbon tetrachloride (CCl_4)-induced hepatotoxicity, and liver regeneration after partial hepatectomy *in vivo* (23–25).

The present study was designed to elucidate the effects of NK2 in CCl_4-induced liver fibrogenesis.

Material and methods

Animals

NK2 transgenic mice were generated on albino FVB genetic background as described previously (23). Expression of human NK2 cDNA was under the control of the mouse metallothionein-1 (MT-1) promoter and associated locus control regions. The construct included the human growth hormone (hGH) polyadenylation site [poly(A)] and the 5′ and 3′ flanking regions of mouse MT genes as described previously (23). Generated NK2 sequences are described previously (18). Mice expressing NK2 generally show no abnormalities except for slight decrease of relative liver weight. But in the present study, no difference was found between NK2 and wild-type (WT) mice livers. WT mice were littermates of NK2 transgenic mice. The animal experiments were conducted in compliance with the guidelines for animal care and use established by Gunma University Graduate School of Medicine. In the fibrosis model, 6-week-old male NK2 transgenic mice ($n=3$) and male WT mice ($n=3$) received intraperitoneal injection of 1 mL/kg CCl_4 (Kanto Chemistry, Tokyo, Japan) dissolved in olive oil (Kanto Chemistry) twice a week. Four weeks after injection (total seven injections), the mice were sacrificed and examined.

Reverse transcriptase polymerase chain reaction assay

NK2 transgene expression in liver tissues was assessed by reverse transcriptase polymerase chain reaction (RT-PCR) assay as described previously (23). Total RNA extraction from the liver tissue and subsequent synthesis of first-strand cDNAs were performed using TRIzol reagent (Invitrogen, Carlsbad, CA, USA) and the SuperScript™ pre-amplification system (Invitrogen) according to the instructions provided by the manufacturer. The cDNAs were amplified using the following primer pairs. MT-S, 5′-ACTCGTCCAACGACTATA-3′, which is specific to the MT-1 promoter region, and GH-A, 5′-AACTTCC AGGGCCAGGAGA-3′, which is specific to the hGH-poly(A) sequence (1019-bp product size). Polymerase chain reaction (PCR) primers were designed to span splice sites in the mRNA to avoid false-positive reactions with chromosomal DNA. Amplification was performed at 94 °C for 40 s, 55 °C for 40 s, 72 °C for 60 s over 35 cycles. The amplified products were electrophoresed in 2% agarose gels and stained with ethidium bromide.

Biochemistry

Serum alanine aminotransferase (ALT) and total bilirubin (T-Bil) levels were measured by routine laboratory methods before and after CCl_4 administration.

Histology

The liver tissue was fixed in 10% formalin, embedded in paraffin and stained with Azan–Mallory (A–M). The extent of fibrosis was quantified with NIH IMAGE ANALYSIS software (v1.62), provided by the National Institute of Health (Bethesda, MD, USA), using three high-power light microscopic fields (×100) per specimen from three mice from each group. The index of fibrosis represented the area of fibrosis divided by the whole area of the microscopic field.

Real-time polymerase chain reaction assay

The mRNA levels of TGF-β1, MMP-13 and HGF were measured using real-time PCR with β-actin as an internal control. Real-time PCR was carried out using the ABI Prism 7700 Sequence Detector and software (Applied Biosystems, Foster City, CA, USA) and the DNA fluorescent dye SYBR Green detection according to the instructions supplied by the manufacturer. Primers were designed using the PRIMER EXPRESS design software (Applied Biosystems). The final result for each sample was normalized relative to the respective β-actin value. Primer sequences were as follows: TGF-β1: 5′-GCCC GAAGCGGACTACTATG-3′ (sense) and 5′-AGATGGC GTTGTTGCGGT-3′ (antisense), MMP-13: 5′-ACT-TAACTTACAGGATTGTGAACTATACTCCT-3′ (sense) and 5′-TGTCAGCAGTGCCATCATAGATT-3′ (antisense) and HGF: 5′-AGAATGGTTCTTGGTGTCATTGT TCC-3′ (sense) and 5′-GATGCTTCAAACACACTG GCC-3′ (antisense).

Western blot analysis

Quantification of α-SMA, c-Met and c-Met tyrosine phosphorylation was performed as described previously (26). Briefly, frozen liver tissue sections were trimmed and total protein from the liver was homogenized in RIPA buffer containing 50 mmol/L Tris (pH 7.4), 50 mmol/L NaCl, 1% Triton X-100, 5 mmol/L ethylenediaminetetraacetic acid, 10 mmol/L sodium PPi (Sigma, St Louis, MO, USA), 50 mmol/L sodium fluoride (Sigma), 1 mmol/L phenylmethylsulphonyl fluoride (Roche Diagnostics, Mannheim, Germany), 10 μg/mL pepstatin (Roche Diagnostics) 10 μg/mL leupeptin (Roche Diagnostics) and 10 μg/mL aprotinin (Roche Diagnostics). Equivalent amounts of lysate were fractionated on a sodium dodecyl sulphate (SDS)-10% polyacrylamide gel (Biocraft, Tokyo), transferred to a polyvinylidene difluoride (PVDF) membrane (Amersham, Buckinghamshire, UK) and incubated with anti-α-SMA antibody (Dako Cytomation, Glostrup, Denmark), anti-c-Met antibody (Santa Cruz Biotechnology, Santa Cruz, CA, USA) and anti-c-Met [$pYpYpY^{1230/1234/1235}$] phosphospecific antibody (BioSource, Camarillo, CA, USA). After incubation with the secondary antibodies corresponding to each antibody, the immunoreactive bands were visualized using an ECL detection system (Amersham) according to the instructions provided by the manufacturer. The intensity of α-SMA, c-Met and c-Met tyrosine phosphorylation bands were normalized to β-actin and values are presented as relative density relative to the control (WT, before CCl_4 administration) using NIH IMAGE ANALYSIS software (v1.62).

Statistical analysis

All experimental data are expressed as mean ± SD. Differences between groups were examined for statistical significance using Student's *t*-test. A *P*-value < 0.05 denoted the presence of a statistically significant difference.

Results

Transgenic mice express NK2 in the liver

High expression of transgene, NK2, was detected in livers of NK2 transgenic mice by RT-PCR, both before and after CCl_4 administration. In contrast, no expression of the transgene was observed in livers of WT mice before or after CCl_4 administration (data not shown).

Extensive liver fibrosis in NK2 transgenic mice

Serum ALT and T-Bil concentrations of NK2 transgenic mice were similar to those of WT mice before CCl_4 administration (ALT: NK2 33.3 ± 11.5, WT 30.0 ± 0 IU/L; T-Bil: 0.3 ± 0.3, WT 0.2 ± 0.1 mg/dL). Five days after the final intraperitoneal injection of CCl_4, serum ALT and T-Bil concentrations in NK2 transgenic mice tended to be higher than in WT mice albeit insignificantly (ALT: NK2 66.7 ± 30.6, WT 36.7 ± 15.3 IU/L; T-Bil: NK2 0.8 ± 0.6, WT 0.3 ± 0.0 mg/dL). These results suggest that the extent of liver injury induced by CCl_4 in NK2 was almost similar to that in WT mice. Histologically, the livers of neither WT mice nor NK2 transgenic mice exhibited any abnormality before CCl_4 administration (Fig. 1A and B). After CCl_4 administration, although WT mice liver showed only mild fibrosis (Fig. 1C), NK2 transgenic mice liver showed bridging fibrosis and nodule formation (Fig. 1D). These results indicated marked liver fibrosis in NK2 transgenic mice compared with WT mice. Quantitative analysis showed that the mean fibrotic area in the livers of NK2 transgenic mice were nine-fold larger than those of WT mice ($P < 0.05$, Fig. 1E).

Expression levels of transforming growth factor-β1, matrix metalloproteinase-13 and α-smooth muscle actin in livers of NK2 transgenic mice

We examined the mRNA expression levels of TGF-β1, MMP-13 and HGF before and after CCl_4 administration in the livers of WT mice and NK2 transgenic mice using real-time PCR. CCl_4 administration increased the expression of TGF-β1 mRNA in livers of NK2 transgenic mice but not of WT mice (Fig. 2A, $P < 0.05$). Moreover, administration of CCl_4 significantly increased the level of TGF-β1 expression in the livers of NK2 transgenic mouse but not in WT mice (Fig. 2A, $P < 0.05$). On the other hand, there was no significant difference in MMP-13 mRNA expression in livers of WT and NK2 mice before CCl_4 administration, but the expression in NK2 livers tended to be lower than in WT livers after CCl_4 administration, albeit insignificantly (Fig. 2B). There was no difference of HGF expression between WT mice and NK2 mice before and after CCl_4 administration (data not shown).

As a marker of activated HSCs, the protein levels of α-SMA were analysed using Western blot analysis. The expression levels of α-SMA in the livers of both WT mice and NK2 transgenic mice were significantly higher after CCl_4 administration than before administration (Fig. 3). Furthermore, CCl_4 administration increased the expression of α-SMA in NK2 livers than in WT livers (Fig. 3).

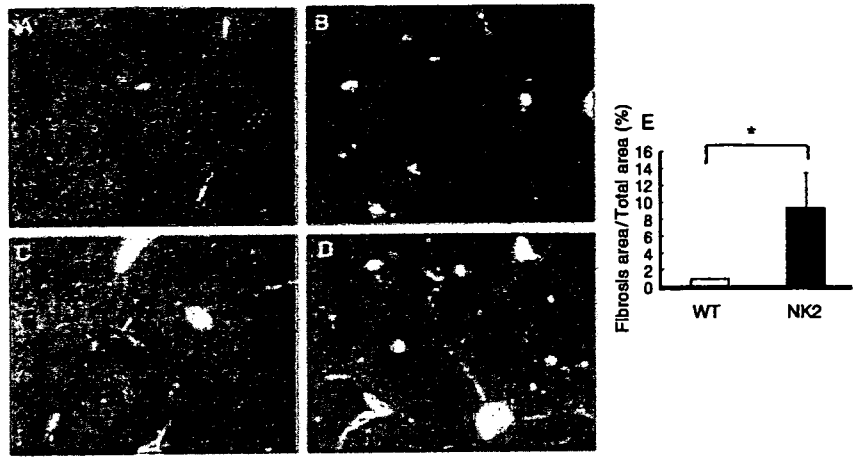

Fig. 1. Histological findings of livers of wild-type mice (A and C) and NK2 transgenic mice (B and D) before CCl_4 administration (A and B) and after CCl_4 administration (C and D). Azan–Mallory staining, × 100. (E) The index of fibrosis represented the area of fibrosis divided by the whole area of the microscopic field. Data are mean ± SD (*$P < 0.05$). CCl_4, carbon tetrachloride.

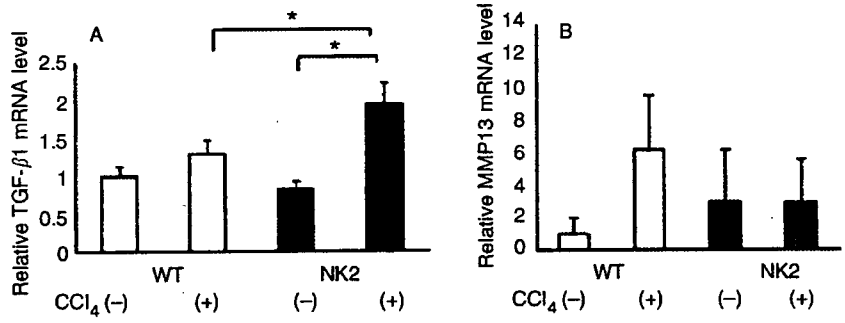

Fig. 2. Real-time polymerase chain reaction analysis of TGF-β1 and MMP-13. Expression of TGF-β1 and MMP-13 mRNAs in livers of WT and NK2 transgenic mice before and after CCl_4 administration. (A) TGF-β1 mRNA expression. (*$P < 0.05$) (B) MMP-13 mRNA expression. CCl_4, carbon tetrachloride; MMP, matrix metalloproteinase; TGF, transforming growth factor; WT, wild type.

Expression of c-Met and activation of c-Met in livers of carbon tetrachloride-treated NK2 transgenic mice

Carbon tetrachloride reduced the expression level of c-Met in both WT mouse livers and NK2 transgenic livers, especially in NK2 (Fig. 4A). Furthermore, CCl_4 administration decreased the level of activated c-Met, detected as the phosphorylated form, although no difference was found between NK2 and WT livers (Fig. 4B).

Discussion

NK2 is a naturally occurring HGF alternative splice variant and acts as an antagonist of HGF *in vitro* (19). We used the NK2 transgenic mouse (23) to investigate the *in vivo* role of NK2, and reported previously that overexpression of NK2 stimulates CCl_4-induced acute liver injury but does not inhibit

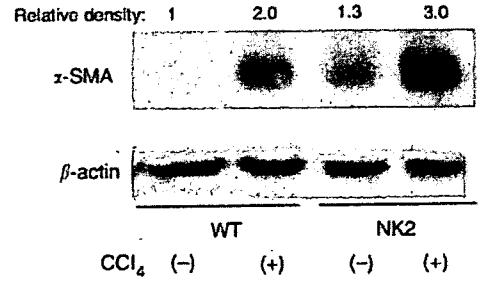

Fig. 3. Western blot analysis of α-SMA. Expression of α-SMA protein in livers of WT and NK2 transgenic mice before and after CCl_4 administration. The intensity of α-SMA bands were normalized to β-actin and values are presented as relative density relative to the control (WT, before CCl_4 administration). CCl_4, carbon tetrachloride; SMA, smooth muscle actin; WT, wild type.

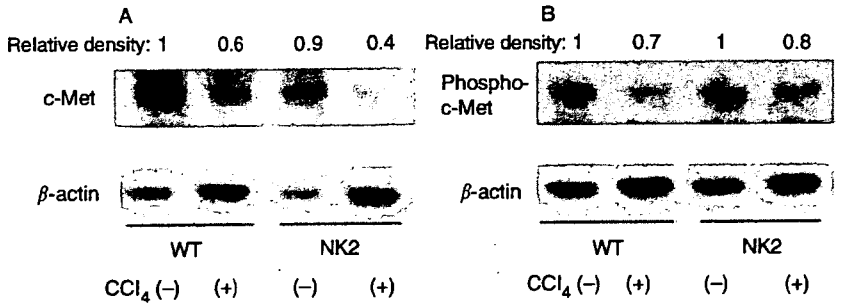

Fig. 4. Western blot analysis of c-Met and phosphorylated c-Met. Expression of c-Met protein and kinase activity in livers of WT and NK2 transgenic mice before and after CCl_4 administration. (A) c-Met protein expression. (B) Phosphorylated c-Met protein expression. The intensity of c-Met and c-Met tyrosine phosphorylation bands were normalized to β-actin and values are presented as relative density relative to the control (WT, before CCl_4 administration). CCl_4, carbon tetrachloride; WT, wild type.

hepatocyte proliferation after CCl_4-induced liver injury in mice (24). In a more recent study, we also demonstrated that overexpression of NK2 inhibits liver regeneration after partial hepatectomy in mice (25). These data indicate that NK2 acts as an antagonist of HGF *in vivo*. In the present study, we investigated the effects of NK2 on CCl_4-induced liver fibrosis using NK2 transgenic mice. HGF administration suppresses the expression of TGF-β1, which is highly associated with hepatic fibrosis and collagen formation (14). HGF inhibits the activation of HSCs, which play a central role in hepatic fibrosis, elicits mitogenic action for hepatocytes and stimulates the expression of MMP (11). These findings could explain the inhibitory effect of HGF in liver fibrogenesis in animal models (14–17). Following CCl_4 administration, NK2 transgenic mice showed marked increase in the severity of liver fibrosis histologically; however, CCl_4 toxicity was not associated with a significant deterioration of liver biochemical function. These results suggest that overexpression of NK2 was not associated with liver damage that resulted in increased fibrogenesis. CCl_4 administration resulted in a significant augmentation of TGF-β1 mRNA expression and an apparently higher induction of α-SMA in NK2 transgenic mouse liver compared with WT mouse liver. On the other hand, CCl_4 resulted in downregulation of MMP-13 in NK2 transgenic mouse liver relative to WT mouse liver. However, HGF expression was unchanged in NK2 transgenic mouse liver after CCl_4 administration. That is, the overexpression of NK2 did not inhibit the expression of HGF. These results indicate that NK2 overexpression promotes CCl_4-induced liver fibrosis *in vivo*, as a manner of the antagonist of HGF.

Hepatocyte growth factor is a heterodimeric glycoprotein consisting of an α-chain, which has an N domain and four kringle domains and a β-chain (5). HGF binds to c-Met and leads to a variety of cellular responses, such as cell survival, proliferation, migration and tubulogenesis. NK2 consists of an N domain and the first two kringle domains of HGF (18). NK2 can bind to c-Met at relatively high affinity and competes with HGF for binding to c-Met (18). In the present study, CCl_4 administration decreased c-Met protein expression in the livers of WT mice and NK2 transgenic mice. This result is similar to the gradual decrease in the hepatic expression of c-Met, reported to occur in parallel with the progression of dimethylnitrosamine-induced rat liver fibrosis (27). In the present study, the expression level of c-Met in NK2 transgenic mouse liver was lower than that in WT mouse liver after CCl_4 administration. This result was compatible with the extent of CCl_4-induced liver fibrosis. CCl_4 also decreased c-Met phosphorylation to a level similar in WT and NK2 transgenic mice. Although NK2 induced c-Met phosphorylation, the biological effects might be different from that induced by HGF; i.e., the qualitative differences between NK2 and HGF could stimulate different types of c-Met-induced downstream signalling. In other words, NK2 can bind and activate c-Met but NK2 may induce different phosphorylation pattern of c-Met and combination of transducers to c-Met from HGF.

In conclusion, our study demonstrated that overexpression of NK2 acts as an antagonist of HGF and promotes liver fibrosis in CCl_4-induced chronic liver injury.

References

1. Nakamura T, Nawa K, Ichihara A. Partial purification and characterization of hepatocyte growth factor from serum of hepatectomized rats. *Biochem Biophys Res Commun* 1984; **122**: 1450–9.